



*Babes-Bolyai University*  
*Faculty of Chemistry and Chemical Engineering,*  
*Department Of Chemistry*



PhD Thesis Abstract

MONICA IRINA REDNIC

**Smart Cyclophanes and Cryptands with Phenothiazine  
Motifs, Anions Sensing with  $\beta$ -HCH and Carbon Dots  
Based Innovative Photoluminescent Materials**

Scientific advisor

**Prof. Dr. Ion Grosu**

Cluj –Napoca

2016





*Babes-Bolyai University  
Faculty of Chemistry and Chemical Engineering,  
Department of Chemistry*



# **Smart Cyclophanes and Cryptands with Phenothiazine Motifs, Anions Sensing with $\beta$ -HCH and Carbon Dots Based Innovative Photoluminescent Materials**

PhD Student

MONICA IRINA REDNIC

Public defense: 20<sup>th</sup> October 2016

## **Thesis Committee:**

President:

**Prof. Dr. Cristian Silvestru**

Babes-Bolyai University, Cluj-Napoca,

Scientific advisor:

**Prof. Dr. Ion Grosu**

Babes-Bolyai University, Cluj-Napoca,

Members:

**Assoc. Prof. Dr. Niculina D. Hădade**

Babes-Bolyai University, Cluj-Napoca,

**Assoc. Prof. Dr. Ileana C. Fărcășanu**

University of Bucharest

**Prof. Dr. Mihail-Lucian Bîrsă**

Alexandru Ioan Cuza University, Iași,

**Cluj –Napoca**

**2016**



## *Table of contents*

*Table of contents*

*List of Abbreviations*

*Keywords*

*Acknowledgements*

*General Introduction*

*Part A. Smart cyclophanes, Cryptands and Supramolecular Architectures with Phenothiazine Motifs*

### **I. Macrocyclic compounds with phenothiazine, acridine, acridane, acridone or phenazine units - literature review**

I.1. Introduction

I.2. Macrocycles with phenothiazine units

I.3. Macrocycles with acridine, acridone or phenazine units

I.4. Conclusions

### **II. Original contributions**

II.1. Introduction

II.2. Podands with 3,7,10-trisubstituted-10*H*- phenothiazine units: synthesis and structural analysis

II.3. Cyclophanes and cryptands with *N*-ethyl-10*H*-phenothiazine bridges

II.3.1. Introduction

II.3.2. Synthesis, structure, and properties of cyclophanes and cryptands with phenothiazine units

II.3.3. Complexations with cations and anions

II.3.4. Cyclic voltammograms of cyclophanes 119 and 120

II.4. Synthesis of new macrocycles with phenothiazine motifs applying dynamic constitutional chemistry

II.4.1. Introduction

II.4.2. Constitutional Dynamic Systems with 10*H*-phenothiazine dialdehydes and bis(aminomethyl)benzenes.

II. 5. Investigation of some protection and deprotection reactions

### **III. Conclusions**

### **IV. Experimental part**

IV.1. General Experimental Data

IV.2. Dipodands: procedures and compounds characterizations

IV.3. Cyclophanes and cryptands: procedures and compounds characterizations

### ***PART B. Anion sensing via $\beta$ -HCH complexes***

#### **I. Introduction**

#### **II. Interactions of $\beta$ -HCH with $\text{Cl}^-$ , $\text{Br}^-$ , $\text{I}^-$ and $\text{HSO}_4^-$**

II.1. Solid state investigations

II.2. Investigations in solution

#### **III. Conclusions**

#### **IV. Experimental data**

IV.1. X-ray data

IV.1.1. Obtaining of single crystals and general experimental conditions

IV.2.  $^1\text{H}$  NMR titration results and ESI-MS data

### ***Part C. Carbon Dots Based Innovative Photoluminescent Materials***

#### **I. Functionalization of CQDs with different organic molecules**

I.1. Introduction

I.2. Objectives

I.3. Grafting CQDs with small molecules

I.4. Functionalization of carbon nanoparticles with oligomers or polymers

I.5. Microwave functionalization of carbon nanoparticles

#### **II. Conclusions**

#### **III. Experimental part**

III.1. Materials

III.2. Measurements

III.3. Carbon nanodots

III.3.1. General Method for the synthesis of functionalized carbon nanoparticles

III.3.2. Functionalization of CQDs with rhodamine (7)

III.3.3. Functionalization of CQDs with isobutyryl bromide(13)

III.3.4. Functionalization of CQD-with oligomers containing carbazole (19)

III.3.5. General Method for the microwave functionalization:

III.3.6. PVK-carbon dots composite films

### ***General Conclusions***

### ***Annexes***

## Keywords

Cyclophanes, Cryptands, Supramolecular Architectures, Anion recognition, Carbon Dots.

## General Introduction

The thesis having the title *Smart Cyclophanes and Cryptands with Phenothiazine Motifs, Anions Sensing with  $\beta$ -HCH and Carbon Dots Based Innovative Photoluminescent Materials* is organized in three parts dealing with the fields of supramolecular chemistry based on macrocyclic host molecules (A), anion sensing (B) and innovative materials (C).

In the first chapter of part A, *Smart Cyclophanes, Cryptands and Supramolecular Architectures with Phenothiazine Motifs*, a careful literature review on the synthesis, structure and properties of macrocycles exhibiting 10-*H*-phenothiazine, acridine, acridane, acridone or phenazine was carried out. In the second chapter, dedicated to the original contributions, the synthesis, structure and binding properties of original cyclophanes and cryptands exhibiting two or three phenothiazine units in the bridges and of their precursors were investigated. The macrocycles were tailored for their synthesis using aromatic nucleophilic substitution reactions and studies concerning their emission properties, in order to reveal the complexation ability of these host molecules for appropriate cations and organic guests, were planned. Complex experiments concerning the possibilities to obtain molecular logical gates based on the emission properties of these compounds were also carried out. In chapter 2 some studies of libraries of compounds obtained in constitutional dynamic experiments and of their evolution towards the more stable products (macrocycles or catenanes) were studied. In the last subchapter of the first part the protection and deprotection of carbonyl groups in the special case of a hindered cryptand was solved. The deprotection (hydrolysis of 1,3-dioxane units) involved the transformation of  $sp^3$  C atoms in  $sp^2$  C atoms leading to a significant increasing of the hindrance in the bridges of the cryptand and producing increased difficulties in the deprotection processes.

In the second part *Anion sensing via  $\beta$ -HCH complexes* the valorization of a cheap and simple molecule ( $\beta$ -HCH) for the detection of anions was presented. The supramolecular recognition of several anions ( $Cl^-$ ,  $Br^-$ ,  $I^-$  and  $HSO_4^-$ ) was investigated either in solid state or in solution. The difacial or monofacial complexation of  $\beta$ -HCH due to important C( $sp^3$ )-H- -anion was investigated in order to support the efficiency of the pattern of 1,3,5-three axial hydrogen atoms on a saturated six-membered ring decorated with electron withdrawing groups for anion recognition. The investigations in solution were carried out by ESI(-)-MS experiments and  $^1H$  NMR titrations. The determination of the stability constants of the complexes of  $\beta$ -HCH with several anions ( $Cl^-$ ,  $Br^-$ ,  $I^-$  and  $HSO_4^-$ ) could be performed.



In the third part *Carbon Dots Based Innovative Photoluminescent Materials* smart materials with exciting photoluminescent properties were prepared and investigated. The primary functionalized C dots were further derivatized with small molecules, oligomers and polymers and the photoluminescent properties of the new materials were investigated by the appropriate methods. The derivatization of C dots based materials was carried out by classic chemical processes or using the microwave activation method.

The scientific results obtained during this thesis were included in five papers, four already published and one of them is submitted.

## Part A. Smart Cyclophanes, Cryptands and Supramolecular Architectures with Phenothiazine Motifs

### I. Macrocyclic compounds with phenothiazine, acridine, acridane, acridone or phenazine units - literature review

### II. Original contributions

#### II.1. Introduction

The literature survey of chapter I revealed the exciting properties of macrocycles exhibiting phenothiazine or other similar aromatic heterocycles. In this context we considered of interest to design, to tailor the synthetic pathway, to synthesize and to investigate the special properties of new macrocycles (coronand like or cryptands) embedding two or more phenothiazine units.

The main targets were podands with phenothiazine motif (V), cyclophanes (VI) and cryptands (VII) exhibiting as reference aromatic groups Nitrogen containing heterocycles and having in the bridges 10*H*-phenothiazine units (Chart 1). Cyclophanes and cryptands showing two or several 10*H*-phenothiazine type linkers might be of interest due to their absorption and emission spectra or due to their electrochemical properties which might be influenced by the electronic communication (including through space) between the heterocycles embedded in the target compounds. The synthetic strategy was inspired by some recent publications<sup>1,2,3,4,5</sup> reporting the successful synthesis of macrocycles and cryptands *via* aromatic nucleophilic substitution reactions starting from diphenols and suitable decorated Nitrogen containing heterocycles. In our work we reacted polyhalogenated 1,3,5-triazine, 1,4-1,3-diazine or pyridine as substrates with 3,7-di(*p'*-hydroxybenzene)-10-ethyl-10*H*-phenothiazine having the role of dinucleophyle.

Another target concerning the phenothiazine based host molecules was connected to the obtaining of macrocycles showing possibilities for further derivatisations. In order to fulfill these conditions we designed and obtained dipodands V (Chart 1) decorated at position 10 (*N*-atom) with -CH<sub>2</sub>-COO*t*C<sub>4</sub>H<sub>9</sub> and -CH<sub>2</sub>-CH<sub>2</sub>-CN groups. These podands were targeted for further investigations envisaging the synthesis of monomeric or dimeric macrocycles exhibiting reactive groups connected to the *N*-atoms of the heterocycles.

---

<sup>1</sup>Hu, W.-J., Zhao, X.-L., Ma, M.-L., Guo, F., Mi, X.-Q., Jiang, B., Wen, K., *Eur. J. Org. Chem.* **2012**, 1448–1454

<sup>2</sup>Kory, M. J., Bergeler, M., Reiher, M., Schlüter, A. D., *Chem. Eur. J.* **2014**, *20*, 6934–6938

<sup>3</sup>Naseer, M. M., Wang, D.-X., Zhao, L., Wang, M.-X., *Eur. J. Org. Chem.* **2014**, 7895–7905

<sup>4</sup>Woiczehowski-Pop, A., Gligor, D., Bende, A., Varodi, C., Bogdan, E., Terec, A., Grosu, I., *Supramol. Chem.*, **2015**, *27*, 52–58

<sup>5</sup>Katz, J.L., Geller, B. J., Conry, R. R., *Org. Lett.*, **2006**, *8*, 2755-2758

On the other hand the high stacking ability of phenothiazine derivatives<sup>6</sup> renders these compounds of interest for DCC (Dynamic Constitutional Chemistry) experiments. In this context we planned to investigate the libraries of compounds issued in the reaction of 1,3-diaminomethylbenzenes in one side with some dialdehydes with phenothiazine moieties on the other side (see Chart 1) and then to evaluate the competition between the formation of macrocycles (*e.g.* dimer macrocycles VIII, formally cyclophanes) and of mechanically interlocked molecules (*e.g.* catenane IX).

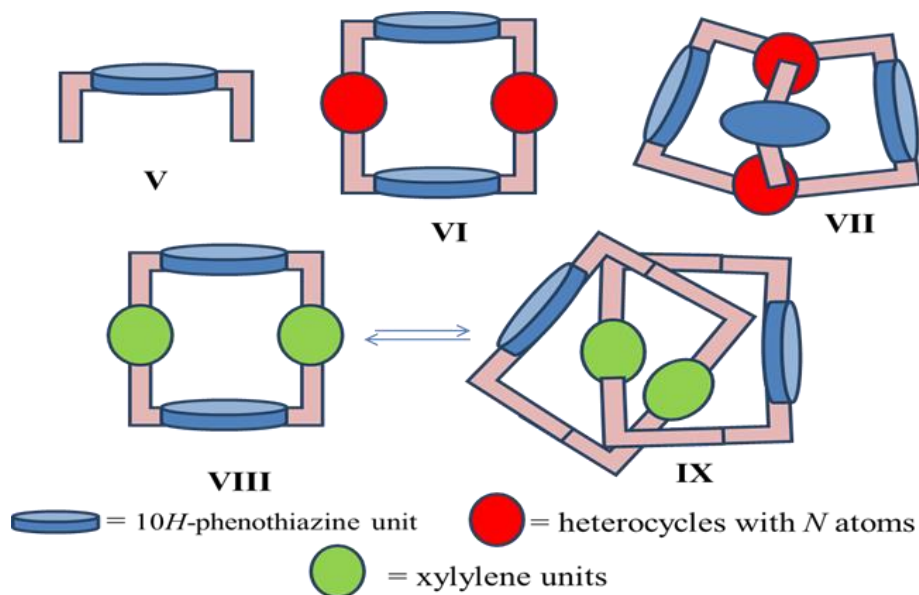


Chart 1. Target dipodands (V), cyclophanes (VI), cryptands (VII) and dynamic libraries (VIII and IX)

## II.2. Podands with 3,7,10-trisubstituted phenothiazine units: synthesis and structural analysis

Phenothiazine based host molecules witnessed an increasing interest. In this context we considered important to develop new synthetic pathways to access phenothiazine based podands decorated with various functional groups. Our target compounds (X-XII, Chart 2) display reactive groups allowing macrocyclisation reactions (-CHO or -CH<sub>2</sub>OH) at positions 3 and 7, and functional groups, at position 10, which can be further used (after deprotection) to connect other relevant entities to the macrocycles or to link to each other several such macrocycles containing phenothiazine moieties (CH<sub>2</sub>COO*t*Bu in X, CH<sub>2</sub>CH<sub>2</sub>CN in XI).

The podands were obtained accordingly to schemes 1-3.

<sup>6</sup>a) **Rednic, M. I.**, Hădade, N. D., Bogdan, E., Grosu, I., *J Incl. Phenom. Macrocycl. Chem.* **2015**, *81*, 263–293.  
 b) Bende, A.; Grosu, I., Turcu, I., *J. Phys. Chem. A*, **2010**, *114*, 12479–12489

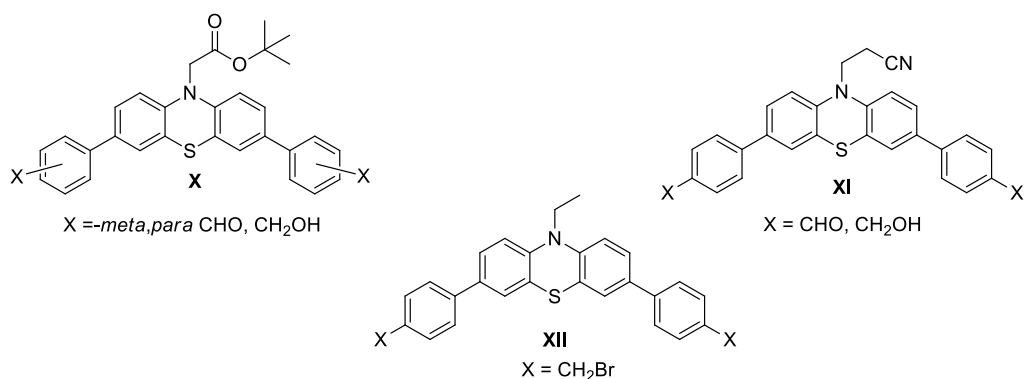
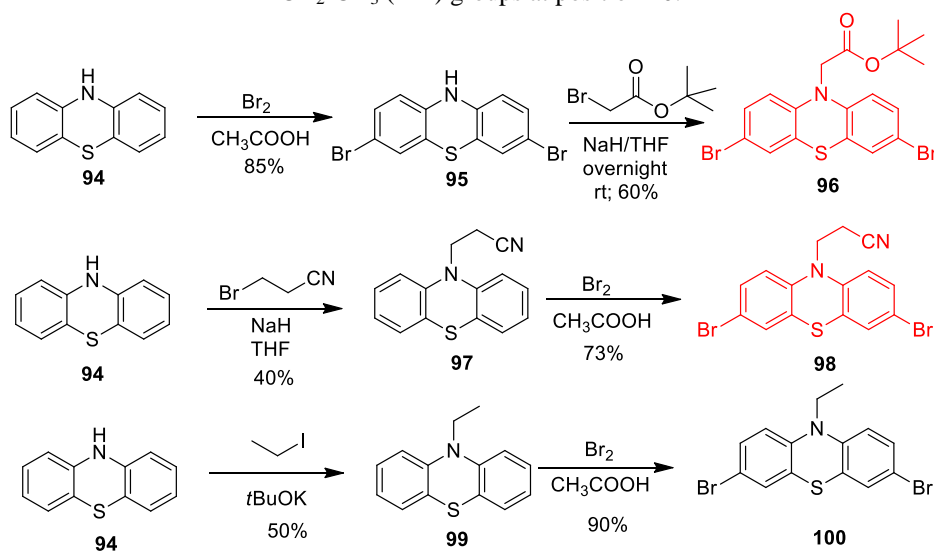
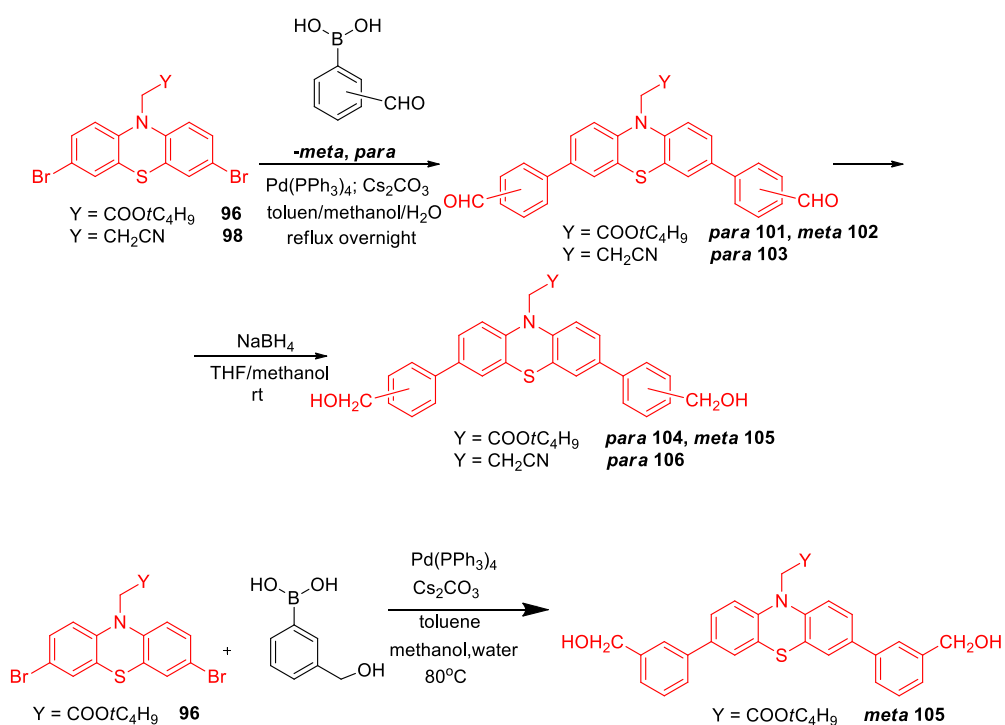


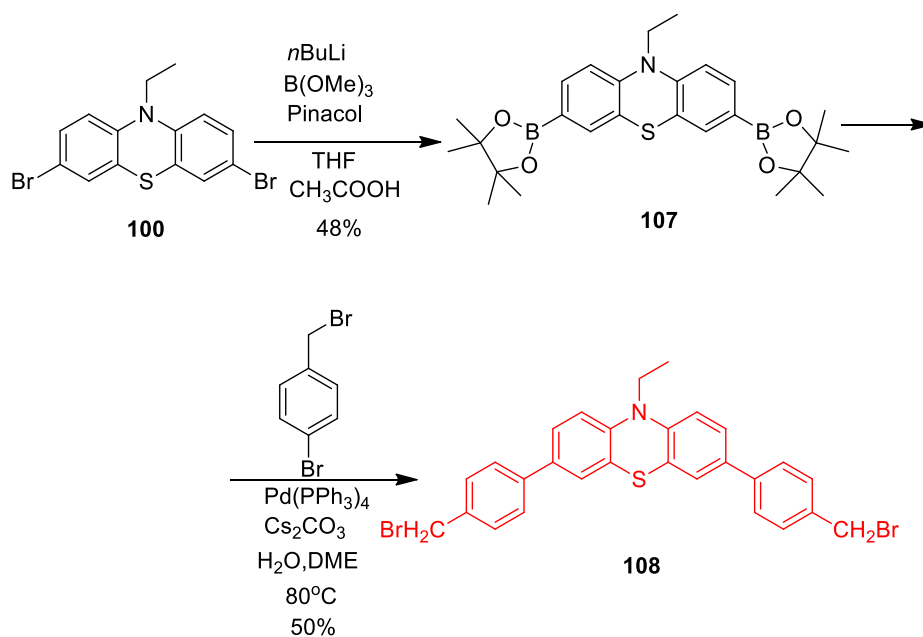
Chart 2. Target phenthiazine based dipodands exhibiting  $-\text{CH}_2\text{COO}t\text{Bu}$  (**X**),  $-\text{CH}_2\text{CH}_2\text{CN}$  (**XI**) and  $-\text{CH}_2-\text{CH}_3$  (**XII**) groups at position 10.



Scheme 1. Synthesis of derivatives **94-100**



Scheme 2. Synthesis of podands **101-106**



Scheme 3. Synthesis of podand **108**

## II.3. Cyclophanes and cryptands with *N*-ethyl-10*H*-phenothiazine bridges

### II.3.1 Introduction

Aromatic nucleophilic substitution reaction became a powerful approach for the access to various macrocycles.<sup>1,2,3,4</sup>

High reactivity of the substrate can be achieved with *N* containing six-membered ring heterocycles ( $\pi$ -deficient aromatic compounds: pyridines, pyrimidines, pyrazines or 1,3,5-triazine) or/and in the case of activated substrates containing electron-withdrawing groups (in *ortho* and *para*, which substantially enhance the rate of substitution) the dihalogenated aromatic compounds.

In this context, we considered of interest to explore the access via aromatic nucleophilic substitution reaction to novel macrocycles (cyclophanes VI or cryptands VII; Chart 2) exhibiting two or more *N*-ethyl-10*H*-phenothiazine units in the bridges and to investigate their electronic and complexation properties.

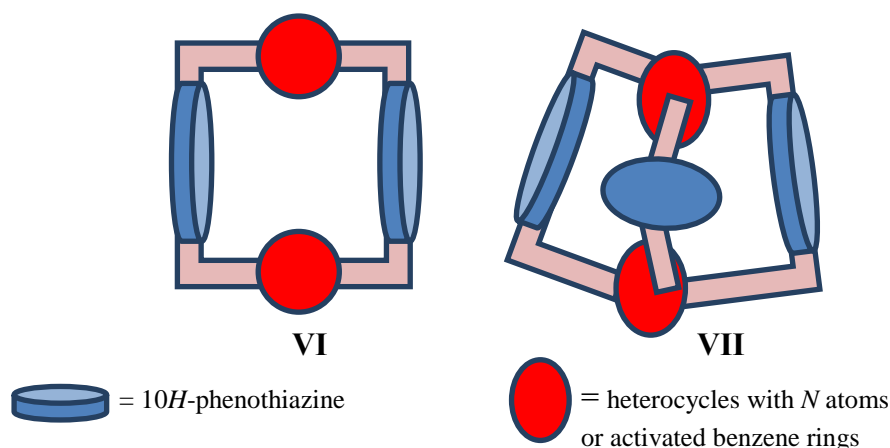
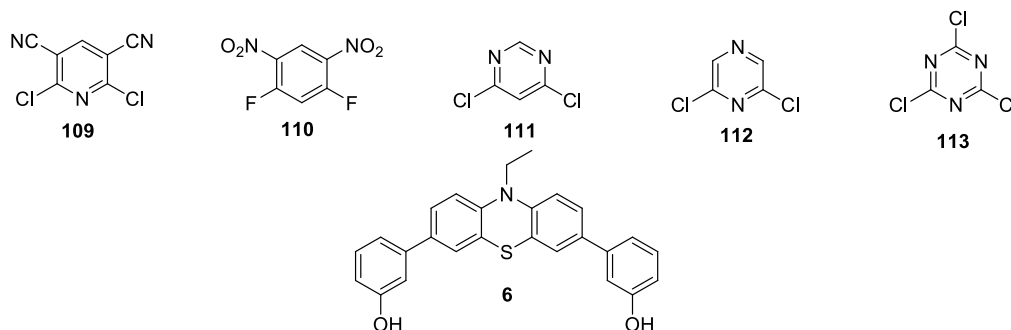


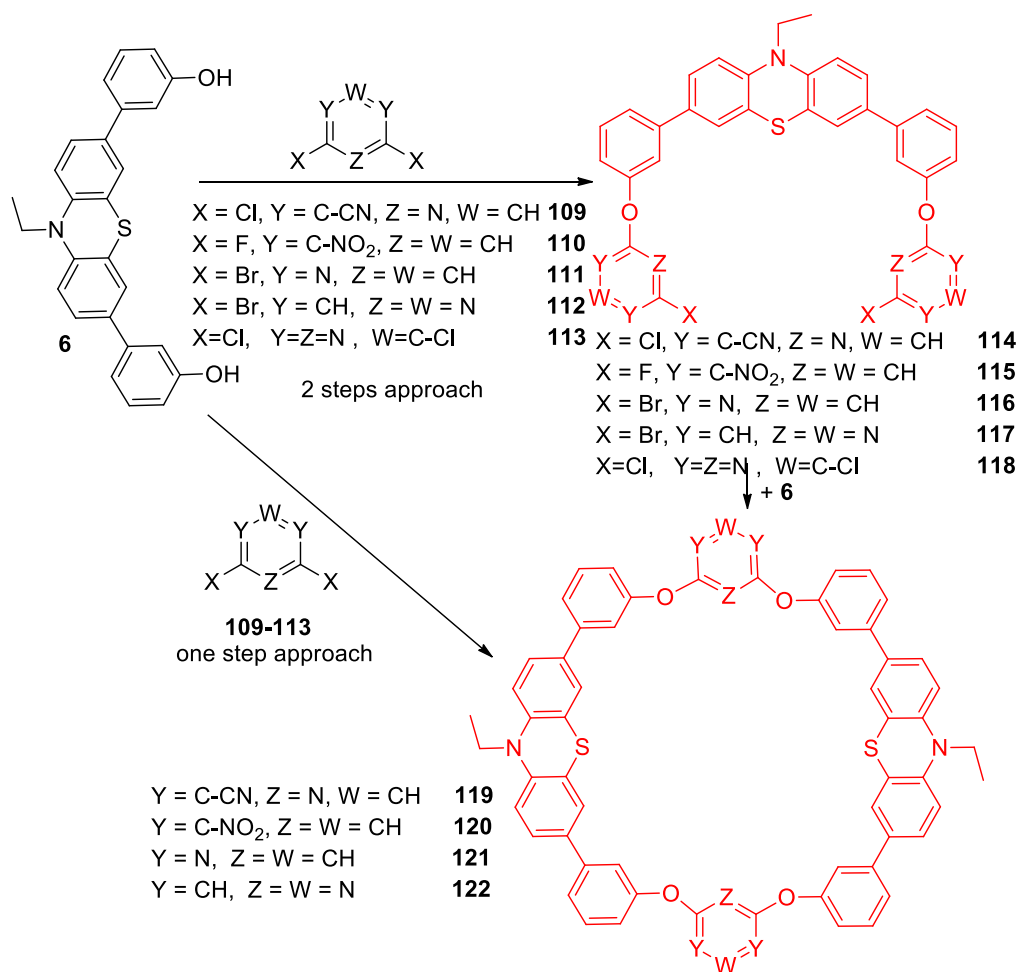
Chart 3. Target cyclophanes (**VI**) and cryptands (**VII**) with 10*H*-phenothiazine units in the bridges

### II.3.2. Synthesis, structure and properties of cyclophanes and cryptands with phenothiazine units

The access to the target macrocycles was based on appropriate substrates **109-113** and 10*H*-phenothiazine nucleophilic reagent **6** (Scheme 4). For the synthesis of cyclophanes **119-123** (Scheme 5) two approaches were taken into consideration: the one step reaction (direct macrocyclization) and a two steps procedure. In the second case, in the first stage was targeted the obtaining (using an excess of substrate) of dipodands **114-118** followed by the macrocyclization using the reaction of these podands with diphenol **6** (Scheme 5).

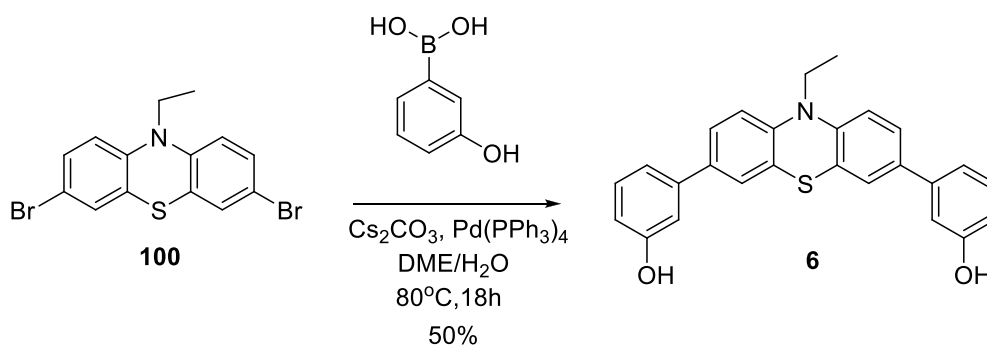


Scheme 4. The main substrates used for obtaining the target macrocycles



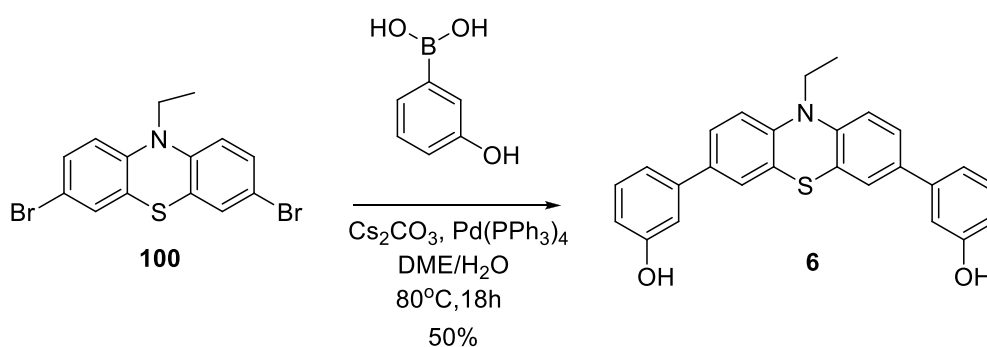
Scheme 5. Synthesis of cyclophanes **119-122**

In order to obtain the desired cyclophanes and cryptands we first synthesized diphenol (**6**) either following a method described in the literature, or using a new procedure elaborated during this work. Thus, in the first method, previously described in the literature, the diboronic diester **107** (obtained from the dibromophenothiazine **100**) was transformed into the precursor **6** by a Suzuki cross coupling reaction with the commercially available *m*-bromo-phenol (Scheme 6).



Scheme 6. Synthesis of diphenol **6**, starting from diboronic diester **107**

In our procedure the roles of bromoaryl and boronic acid are changed. Dibrominated derivative **100** was reacted with (3-hydroxyphenyl)boronic acid in the presence of an excesses of cesium carbonate in a mixture of solvents DME/H<sub>2</sub>O = 2/1 and palladium tetrakis(triphenylphosphine) as catalyst and gave in one step the target diphenol **6** (Scheme 7).



Scheme 7. One step access to diphenol **6**

The procedures for the one pot reaction (diphenol **6** and substrates **109-113** in 1/1.1 ratio) and for the macrocyclization phase in the two steps approach (intermediates **114-118** in reaction with nucleophile **6** in 1/1.1 ratio) were similar. Optimizations of the reaction conditions were necessary for the construction of macrocycles **119-122**. The reaction conditions were varied and the efficiency of the reactions was monitored. Combinations of bases and solvents and different reaction temperatures revealed the important role of these conditions in directing the course of the synthesis (Table 1).

Table 1. Results of different strategies for obtaining cyclophanes **119-122**

Cyclophanes	Procedure A (one pot reactions)					Procedure B (with intermediate)				
	Bases	Solvents	t (°C)	t (h)	Yield (%)	Bases	Solvents	t (°C)	t (h)	Yield
<b>119</b>	NEt <sub>3</sub>	DMSO	80	24	31	DIPEA	THF	40	24	-
	-	-	-	-	-	DIPEA	1,4-dioxane	80	24	-
	-	-	-	-	-	NEt <sub>3</sub>	DMSO	80	48	39
<b>120</b>	NEt <sub>3</sub>	DMSO	80	24	17	NEt <sub>3</sub>	DMSO	80	24	33
<b>121</b>	Cs <sub>2</sub> CO <sub>3</sub>	DMSO	120	24	20	Cs <sub>2</sub> CO <sub>3</sub>	DMSO	120	24	24
<b>122</b>	Cs <sub>2</sub> CO <sub>3</sub>	DMSO	120	24	11	Cs <sub>2</sub> CO <sub>3</sub>	DMSO	120	48	21

Intermediates play an important role in the synthesis of macrocycles **119-122** through procedure B (two steps) and we focused on their efficient synthesis. For the obtaining the intermediates **114-118** we used nucleophile **6** and substrates **109-113**, in a 1/5 molar ratio.

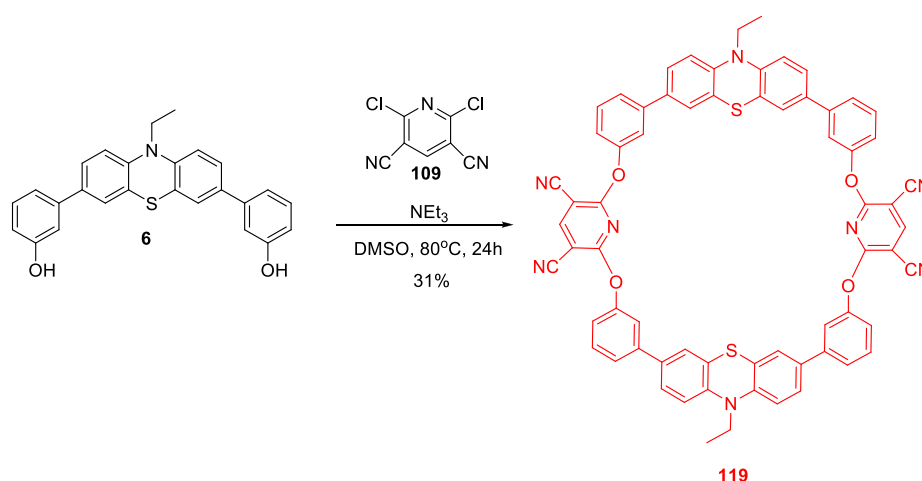


The experiments were carried out with various bases, solvents and for different reaction times. Some comments are necessary to be mentioned if we compare the data of the two tables (1 and 2). The intermediate **114** was obtained with a good yield (65%) using THF as a solvent and DIPEA as a base, but for the synthesis of cyclophane **119** (procedure B, see table 1) in the same conditions the reaction failed.

Table 2. Results for the synthesis of intermediates **114-118**

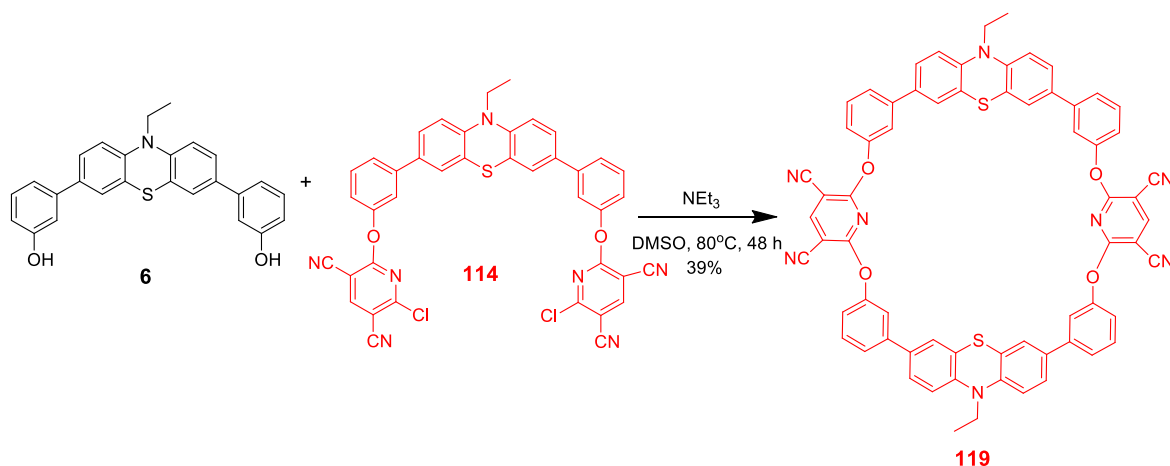
Intermediates	Conditions reactions				
	Bases	Solvents	t(°C)	t (h)	Yield
<b>114</b>	DIPEA	THF	40	72	65
<b>115</b>	NEt <sub>3</sub>	DMSO	80	48	41
<b>116</b>	Cs <sub>2</sub> CO <sub>3</sub>	DMSO	120	48	52
<b>117</b>	Cs <sub>2</sub> CO <sub>3</sub>	DMSO	120	24	33
<b>118</b>	DIPEA	THF	40	24	50

The reaction of **6** with **109** in a 1:1.1 molar ratio in DMSO in the presence of triethylamine afforded **119** in a 31% yield (Scheme 8).



Scheme 8. One pot synthesis of macrocycle **119**

The yields of the reaction of **6** with **114** varied depending on the employed conditions (Table 3). As indicated in table 2, when DIPEA was used as base, the reaction in THF or 1,4-dioxane at 40°C or 80°C, respectively gave traces of the desired cyclophane **119**. If the solvent was changed to dimethylsulfoxide and the base to triethylamine the reaction carried out at 80°C gave the desired compound in 39% yield (Scheme 9).

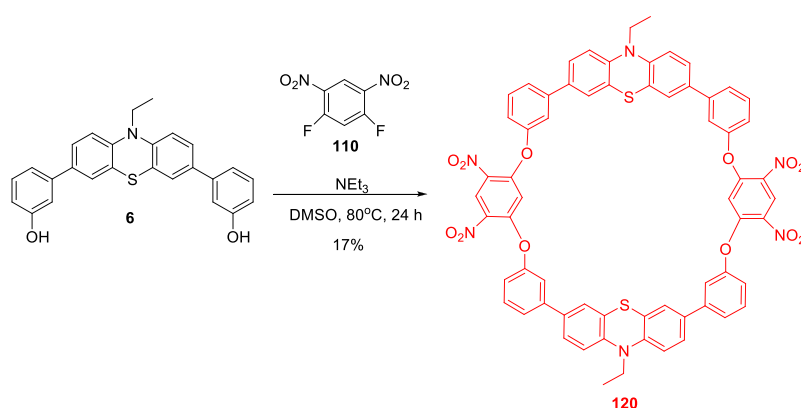


Scheme 9. Synthesis of macrocycle **119** by the reaction of **6** with intermediate **114**

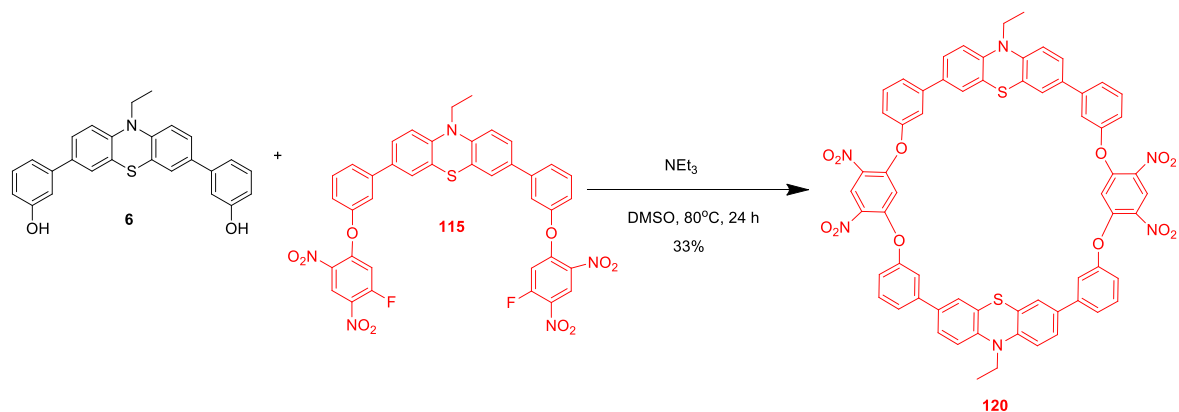
Table 3. Results of the synthesis of cyclophane **119** by aromatic nucleophilic substitution reaction between **6** and **114** in various reaction conditions

Solvent	Base	Temperature (°C)	Yields
THF	DIPEA	40	Traces
1,4-dioxane	DIPEA	80	Traces
DMSO	NEt <sub>3</sub>	80	39 %

In the case of the reaction of 1,5-difluoro-2,4-dinitrobenzene (**110**) with diphenol (**6**) through the one pot procedure the expected cyclophane **120** was obtained in 17 % yield (Scheme 10). The reaction of intermediate **115** with diphenol **6** in the presence of triethylamine as base and dimethylsulfoxide as solvent the yield (33%, Scheme 11) was considerably better.

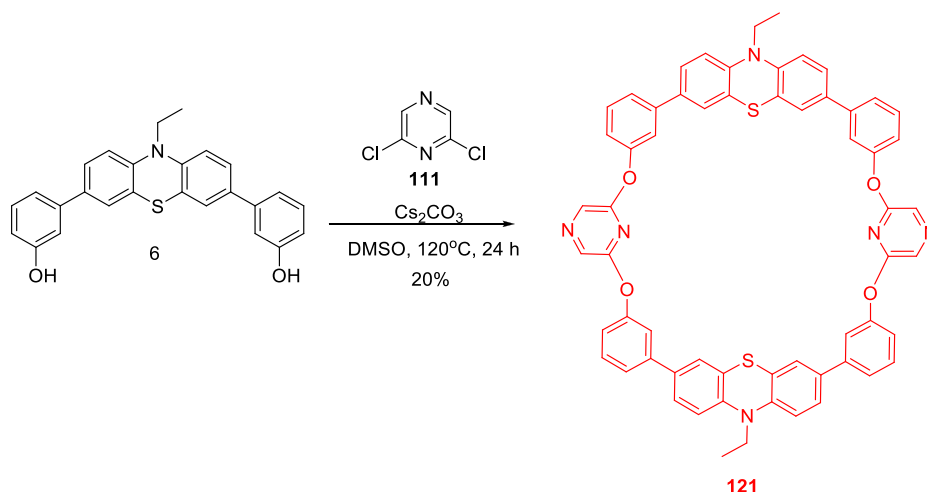


Scheme 10. Synthesis of macrocycle **120** by “one pot” procedure

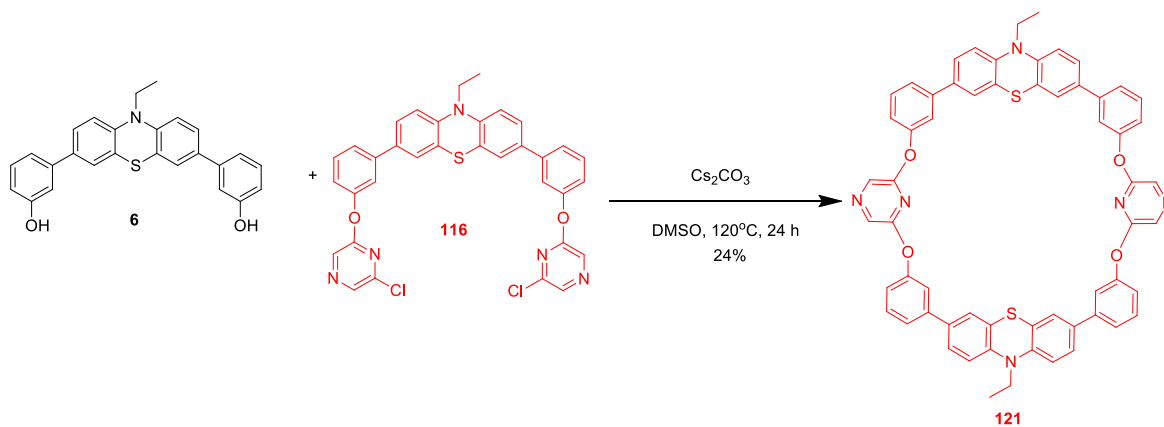


Scheme 11. Synthesis of macrocycle **120** by the reaction of **6** with intermediate **115**

Cyclophane **121** was obtained by one pot reaction from nucleophile **6** and electrophile 2,6-dichloropyrazine in DMSO in the presence of  $\text{Cs}_2\text{CO}_3$  as base, at  $120^\circ\text{C}$ , in 20% yield. The reaction of **6** with intermediate **116** in similar conditions gave the target cyclophane in 24% yield (Scheme 12).

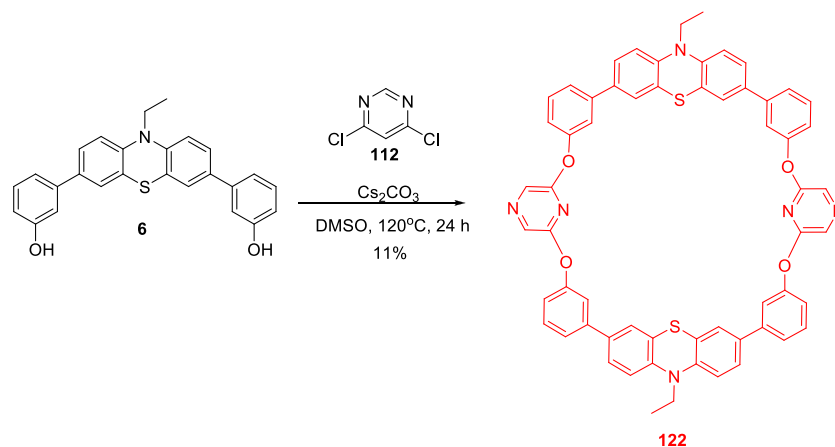


Scheme 12. One pot synthesis of cyclophane **121**

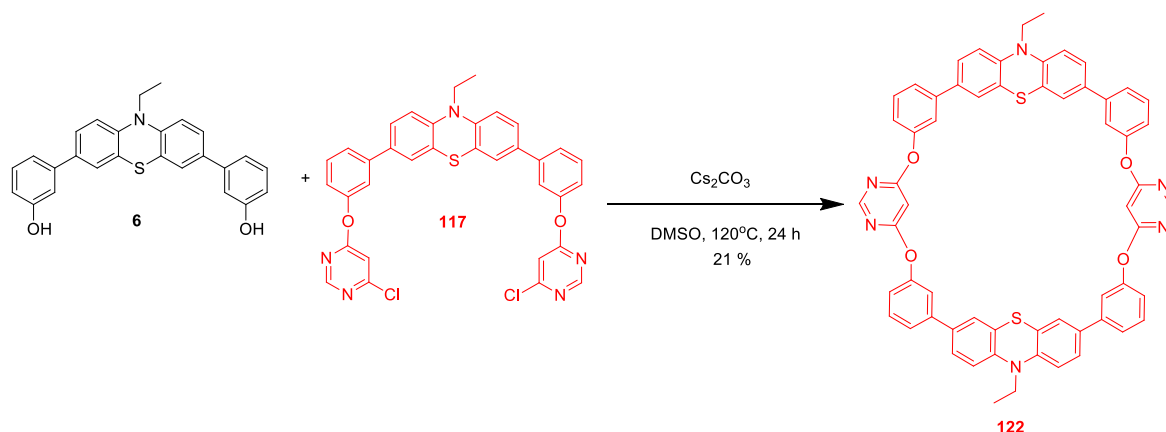


Scheme 13. Synthesis of macrocycle **121** by the reaction of **6** with intermediate **116**

The macrocyclization reaction using 4,6-dichloropyrimidine as substrate gave in the one pot strategy cyclophane **122** in 11% yield (Scheme 14), while in the case the two steps procedure the ring closure using intermediate **117** led to cyclophane **122** in 21% yield (Scheme 15).



Scheme 14. One pot synthesis of **122**



Scheme 15. Synthesis of cyclophane **122** by the reaction of **6** with intermediate **117**

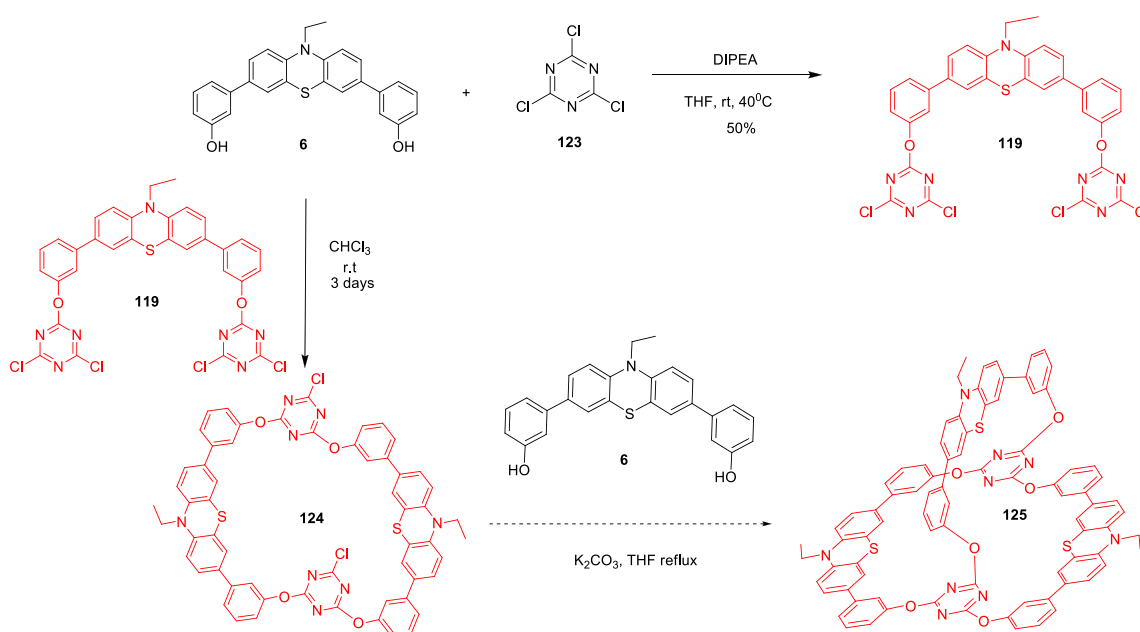
The strategy for the obtaining of cryptand **125** (having as substrate the cyanuric chloride) was inspired from literature data.<sup>1,6</sup> Cyanuric chloride presents a remarkable difference of the reactivity of the three chlorine atoms if their replacement is carried out *step by step*. In this context, the application of a three steps strategy based on step by step formation of the three bridges of the cryptand was considered worthy, ensuring a permanent control over the reactions.

The three steps for the formation of cryptand **125** are presented in scheme 16. The synthesis started from diphenol **6** which was reacted with cyanuric chloride in a 1:5 molar ratio in order to obtain podand **119** (40°C, THF, Hünig's base). The next step was the transformation of intermediate **119** in cyclophane **124** employing a 1:1.1 molar ratio

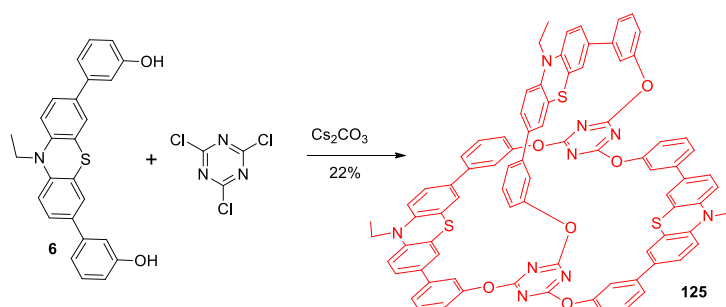
podand/nucleophile (anhydrous  $\text{CHCl}_3$ , DIPEA, at *r.t.* for 3 days). In the final step, the attachment of the third bridge was planned to be carried out under dilution, at reflux of THF, and having  $\text{K}_2\text{CO}_3$  as base and a stoichiometric ratio substrate / nucleophile.

Unfortunately, the multistep strategy failed because of the low yields for the synthesis of dipodand **119**, so compound **124** was obtained in insufficient amounts for a successful run of the third step.

In these conditions we decided to carry out a “one step” procedure using the direct reaction of cyanuric chloride with diphenol **6** in high dilution, in a 2/3 ratio employing the conditions which were successful for the one step synthesis of cyclophanes **119-122** (Scheme 17).



Scheme 16. The three steps synthesis of cryptand **125**



Scheme 17. The one step synthesis of cryptand **125**

All the new synthesized compounds were investigated through NMR Spectroscopy ( $^1\text{H}$ ,  $^{13}\text{C}$ , COSY) and High Resolution Mass Spectrometry (HRMS). The  $^1\text{H}$  NMR spectra revealed the number of signals corresponding to the structure of target compounds. In

aromatic area we have identified the characteristic signals for symmetrically 3,7-disubstituted-10*H*-phenothiazine units.

The  $^1\text{H}$  NMR spectra of intermediate **115** and cyclophane **120** exhibit in the aliphatic area two signals, one triplet corresponding to methyl group at 1.33 ppm for **115** (1.28 ppm for **120**) and a quartet corresponding to methylene protons at 3.98 for **115** (3.79 for **120**) ppm.

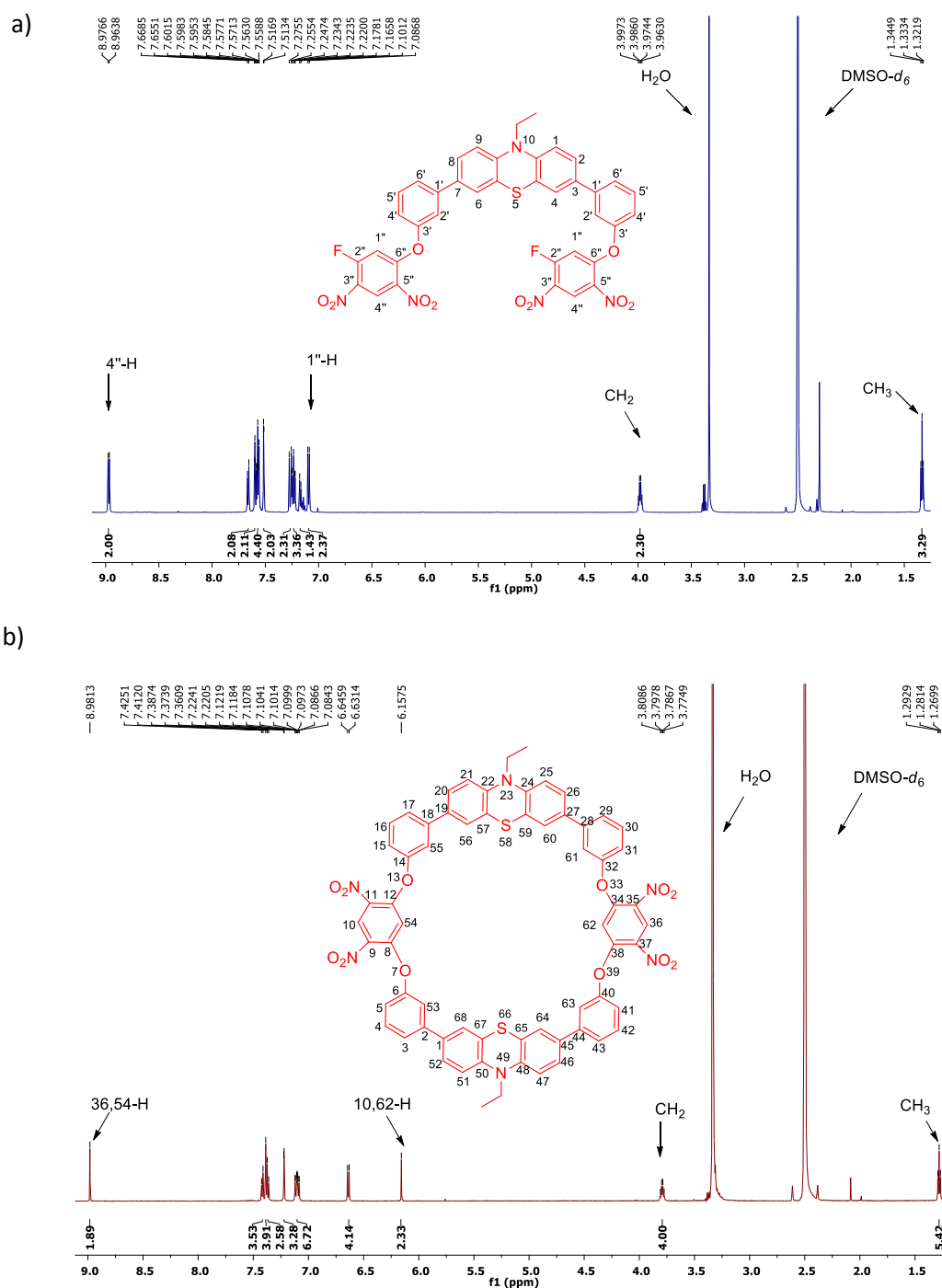
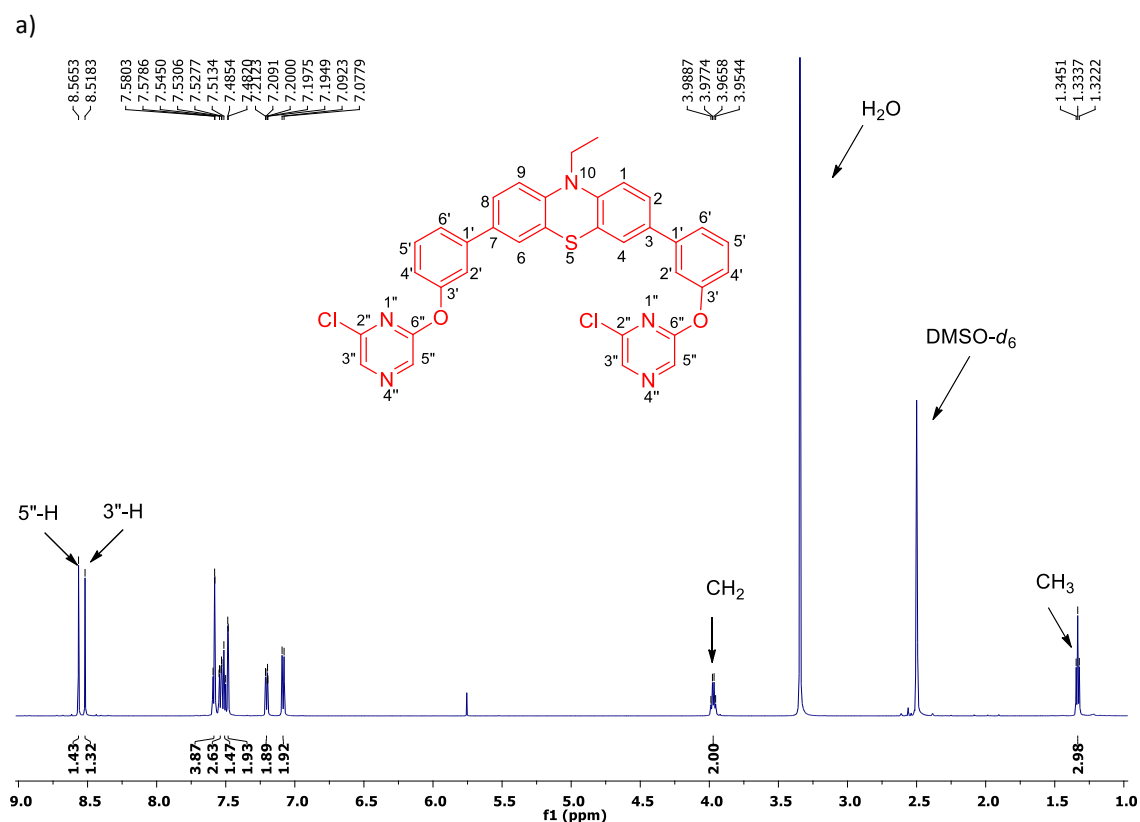


Figure 1.  $^1\text{H}$  NMR (600 MHz,  $\text{DMSO-}d_6$ ) spectra (fragments) of intermediate **115** (a) and cyclophane **120** (b)

Differences in the spectra of these compounds appear in aromatic signals area, where in the case of intermediate **115**, along with the signals pertaining to the classic pattern of 3,7-disubstituted-10*H*-phenothiazine, we have encountered two doublets (Figure 1a) for the protons at positions 4'' ( $\delta = 8.97$  ppm,  $J = 7.7$  Hz) and 1'' ( $\delta = 7.09$  ppm,  $J = 8.6$  Hz). The multiplicity of these signals is due to the heteronuclear coupling with the adjacent fluor atoms. In the  $^1\text{H}$  NMR spectrum of cyclophane **120** the similar protons (positions 10, 36 and 54, 62) give two singlets [ $\delta = 8.98$  and 6.16 ppm, Figure 1b)].

In figure 2 are shown relevant fragments of  $^1\text{H}$  NMR spectra of intermediate **116** (Figure 2a) and cyclophane **121** (Figure 2b). The spectrum of cyclophane **121** presents in the aromatic area a singlet for the protons at positions 9, 11, 35 and 37 ( $\delta = 8.30$  ppm), and a group of signals (two doublets, two doublets of doublets, one triplet, and two overlapped doublets) which can be assigned to the pattern of 3,7-disubstituted-10*H*-phenothiazine moiety. In the aliphatic signals area the ethyl group displays a quartet ( $\delta = 3.66$  ppm) and a triplet ( $\delta = 1.21$  ppm).



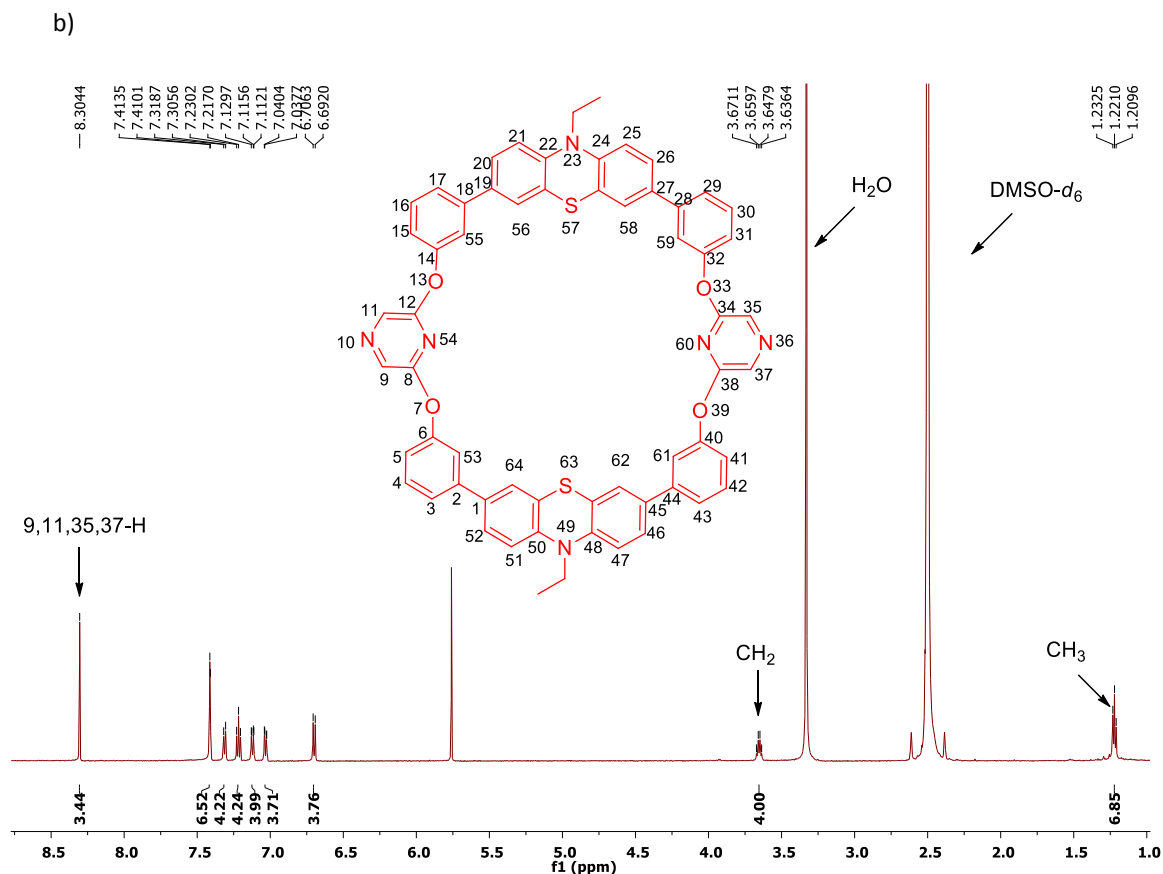


Figure 2.  $^1\text{H}$  NMR spectra (fragments) of intermediate **116** (a) and cyclophane **121** (b)

The intermediate **116** has in the aromatic zone two singlets for the protons at positions 3'' ( $\delta = 8.52$  ppm) and 5'' ( $\delta = 8.57$  ppm) and the classic pattern of signals for the protons of phenothiazine unit. In the spectrum of cyclophane **121** for the similar protons (positions 9, 11, 35, 37) only a singlet ( $\delta = 8.30$  ppm) was recorded.

The  $^1\text{H}$  NMR and  $^{13}\text{C}$  NMR spectra of cryptand **125** (Figures 3 and 4) exhibit a reduced number of signals due to the high symmetry of the compound (proving the obtaining of the target cryptand). The  $^1\text{H}$  NMR spectrum displays only seven clear signals for the aromatic protons which correspond to the 3,7-disubstituted-10-ethyl-10*H*-phenothiazine part (three signals for the heterocycle and four signals for the *meta* disubstituted benzene units) and the quartet and triplet belonging to the protons of the ethyl groups. The  $^{13}\text{C}$  NMR spectrum reveals for the aromatic carbon atoms seven signals for tertiary and five signals for the quaternary carbon atoms. The two signals belonging to the ethyl groups can be observed in the aliphatic region of the spectrum.



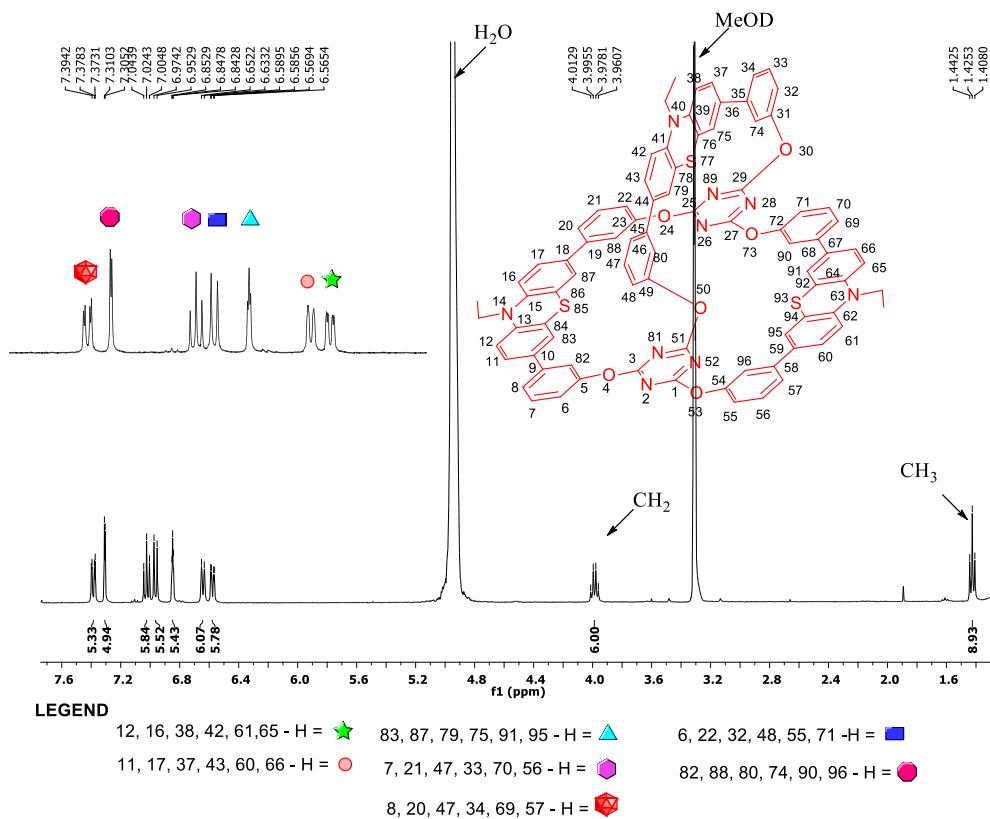


Figure 3.  $^1\text{H}$  NMR (600MHz,  $\text{CD}_3\text{OD}$ ) (fragment) spectrum of cryptand **125**

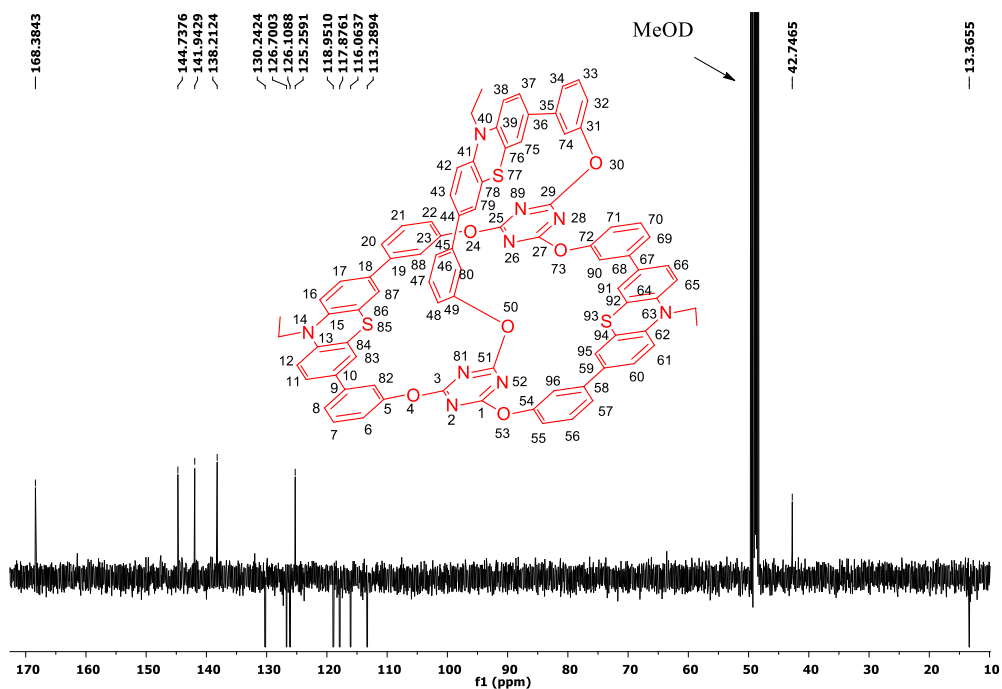
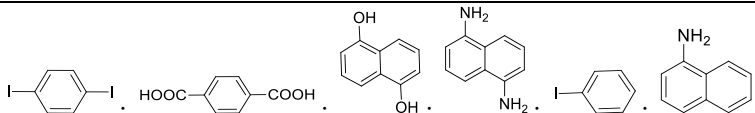


Figure 4.  $^{13}\text{C}$  NMR (150 MHz,  $\text{CD}_3\text{OD}$ ) (fragment) spectrum of cryptand **125**

### II.3.3. Complexations with cations and anions

Due to macrocyclic cavity, cyclophanes with phenothiazine moiety are acting as hosts molecules for different cationic or anionic guests. In the interest of evaluate guest-binding ability with cyclophanes **119**, **120**, **121** as hosts a number of transitional metals salts and organic molecules (Table 4) as guests were investigated by spectroscopic methods and by electrochemical measurements.

Table 4. Guest molecules

<b>Transitional metals salts</b>	$\text{Cd}(\text{NO}_3)_2$ ; $\text{Co}(\text{NO}_3)_2$ ; $\text{Pb}(\text{NO}_3)_2$ ; $\text{CdSO}_4$ ; $\text{CoSO}_4$ ; $\text{Cd}(\text{OAc})_2 \cdot 2\text{H}_2\text{O}$ ; $\text{Pb}(\text{OAc})_2 \cdot 3\text{H}_2\text{O}$ ; $\text{Zn}(\text{OAc})_2 \cdot 2\text{H}_2\text{O}$
<b>Organic molecules</b>	

All cyclophanes exhibited absorption maxima at about 280 nm (Figure 5) and emission bands between 470-485 nm (Figure 6).

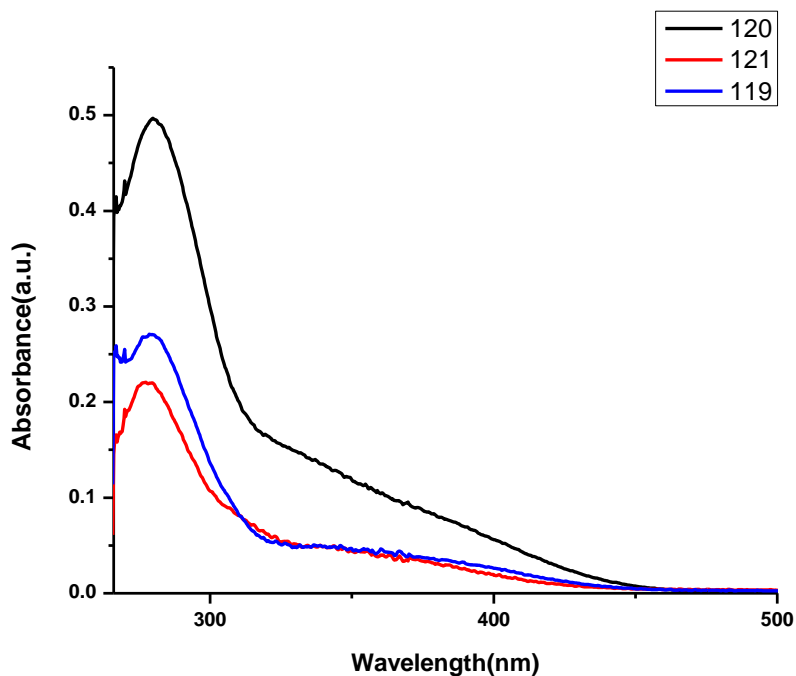


Figure 5. UV-VIS absorbance spectra of **119** (blue), **120** (black) and **121** (red)

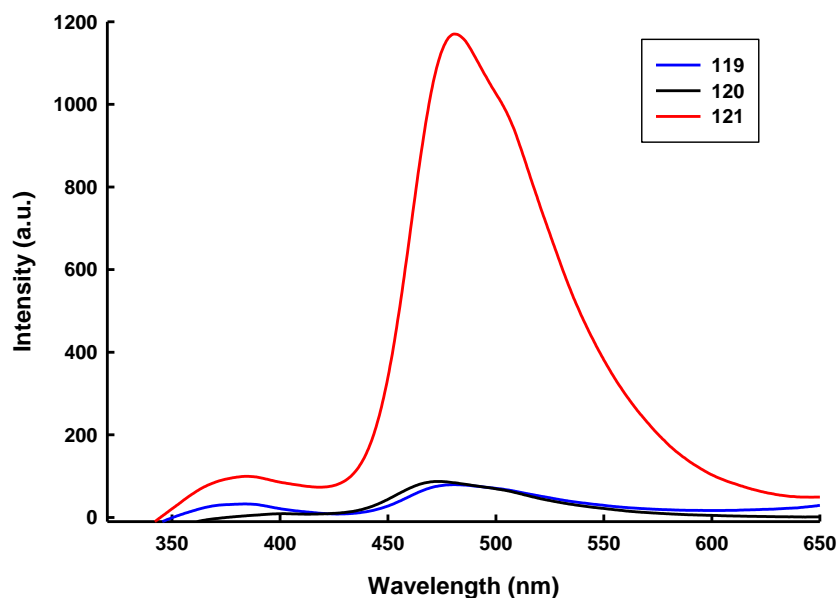


Figure 6. Emission spectra of **119** (blue), **120** (black), **121** (red)

The complexation with transitional metal salts and organic molecules was studied by adding equal amounts of solution of organic compounds or inorganic ions to a solution of the same concentration of the studied cyclophanes. In all cases the concentration of cyclophanes was kept constant at  $1.65 \times 10^{-6}$  M in DMF as solvent. The solutions were subjected to ultrasonic waves for 3 min for homogenization.

Figure 7 illustrates the fluorescence spectra of cyclophane **119** in the presence of  $\text{Cd}^{2+}$ ,  $\text{Co}^{2+}$ ,  $\text{Pb}^{2+}$  nitrate salts. The value (17.82) of intensities ratio ( $I_{\text{complex}}/I_{119}$ ) for the complex with  $\text{Co}^{2+}$  is higher than the value (9.30) of the intensities ratio ( $I_{\text{complex}}/I_{119}$ ) in the case of the complex with  $\text{Pb}^{2+}$  (Table 5).

Table 5. UV-Vis and fluorescence spectroscopy data [(s):  $\sim 1.65 \times 10^{-6}$  M in DMF] of **119** with cations of nitrates salts

Samples	$\lambda_{\text{max}}$ (s) [nm]	$\epsilon_{\text{max}}$ [ $\text{M}^{-1}\text{cm}^{-1}$ ]	$\lambda_{\text{em}}$ (s) [nm]	$I_{\text{em}}$ [a.u.]	$I_{\text{complex}}/I_{119}$
<b>119</b>	280	81818	482	79	
<b>119 +</b> <b>Cd(NO<sub>3</sub>)<sub>2</sub></b>	279	71560	477	222	2.8
<b>119 +</b> <b>Co(NO<sub>3</sub>)<sub>2</sub></b>	280	62289	477	1408	17.82
<b>119 +</b> <b>Pb(NO<sub>3</sub>)<sub>2</sub></b>	280	71348	476	735	9.30

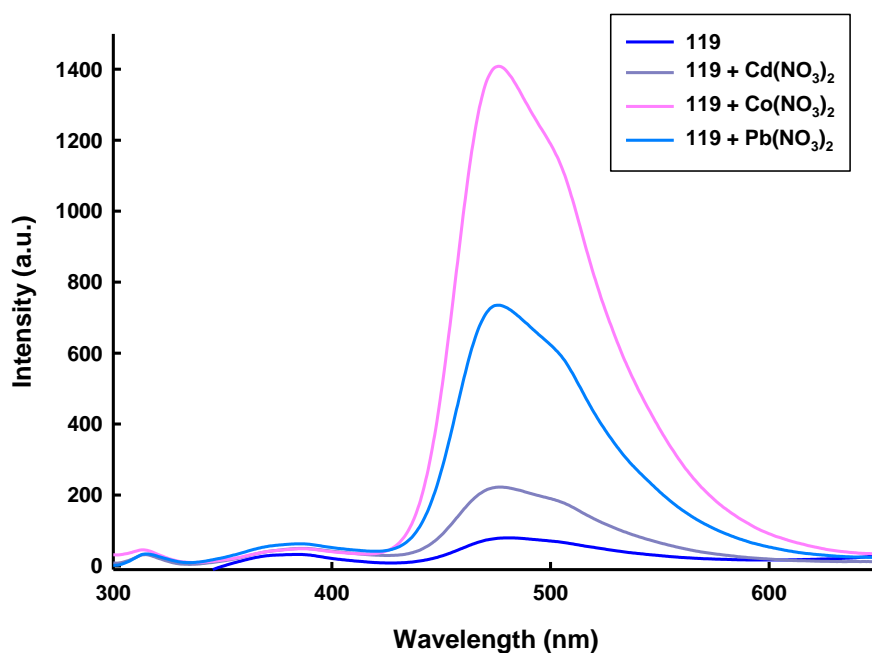


Figure 7. Fluorescence spectra of cyclophane **119** in the presence of various cations of nitrate salts ((s):  $\sim 1.65 \times 10^{-6}$  M in DMF)

It is interesting to notice that complexation with iodobenzene increased the fluorescence intensity of the host by a factor of 73, while in the case of aminonaphthalene fluorescence intensity is increased by a factor of 56. Surprisingly, when the organic guests are added together the emission intensity decreased as compared with the case when only one guest is used, but it is increased by a factor of 47 when it is compared with the spectrum of free host **119** (Table 6).

Table 6. UV-Vis and fluorescence spectroscopy data ((s):  $\sim 1.65 \times 10^{-6}$  M in DMF)) of **119** in the presence of iodobenzene and aminonaphthalene.

Samples	$\lambda_{\max}$ (s) [nm]	$\epsilon_{\max}$ [ $M^{-1}cm^{-1}$ ]	$\lambda_{em}$ (s) [nm]	$I_{em}$ [a.u.]	$I_{complex}/I_{119}$
<b>119</b>	280	81818	482	79	
<b>119 + iodobenzene</b>	268	102463	490	5745	73
<b>119 + aminonaphthalene</b>	278	117730	476	4462	56
<b>119 + iodobenzene+aminonaphthalene</b>	278	79458	476	3760	47

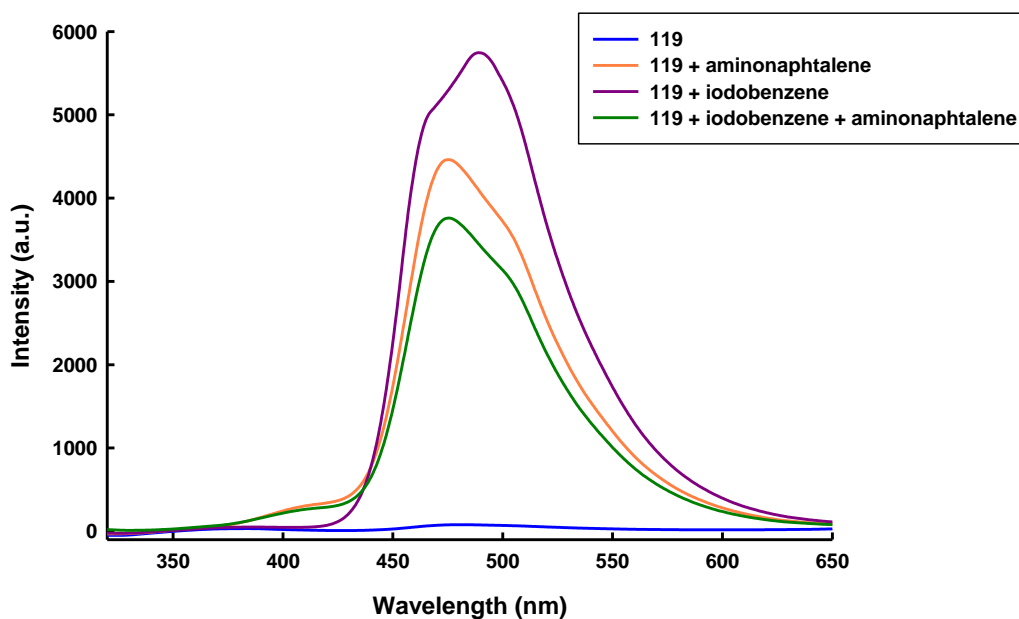


Figure 8. Fluorescence spectra of cyclophane **119** in the presence of iodobenzene and aminonaphthalene and the mixture of the two guests [(s):  $\sim 1.65 \times 10^{-6}$  M in DMF]

A similar behavior of the emission spectra intensities was observed in the systems formed by cyclophane **120** with inorganic cations.

The complexation of cyclophane **120** with  $\text{Pb}^{2+}$  increased the fluorescence intensity by a factor of 11 and with  $\text{Cd}^{2+}$  by a factor of 7.6, while when both cations are added the intensity factor decreased to 1.2 (Table 7)

Table 7. UV-Vis and fluorescence spectroscopy data ((s):  $\sim 1.65 \times 10^{-6}$  M in DMF)) of **120** in the presence of some nitrate salts

Samples	$\lambda_{\text{max}}$ (s) [nm]	$\epsilon_{\text{max}}$ [ $\text{M}^{-1}\text{cm}^{-1}$ ]	$\lambda_{\text{em}}$ (s) [nm]	$I_{\text{em}}$ [a.u.]	$I_{\text{complex}}/I_{120}$
<b>120</b>	280	151515	473	87	
<b>120</b> + $\text{Cd}(\text{NO}_3)_2$	280	91024	473	661	7.6
<b>120</b> + $\text{Pb}(\text{NO}_3)_2$	280	97521	473	956	11
<b>120</b> + $\text{Cd}(\text{NO}_3)_2$ + $\text{Pb}(\text{NO}_3)_2$	280	78715	472	112	1.2

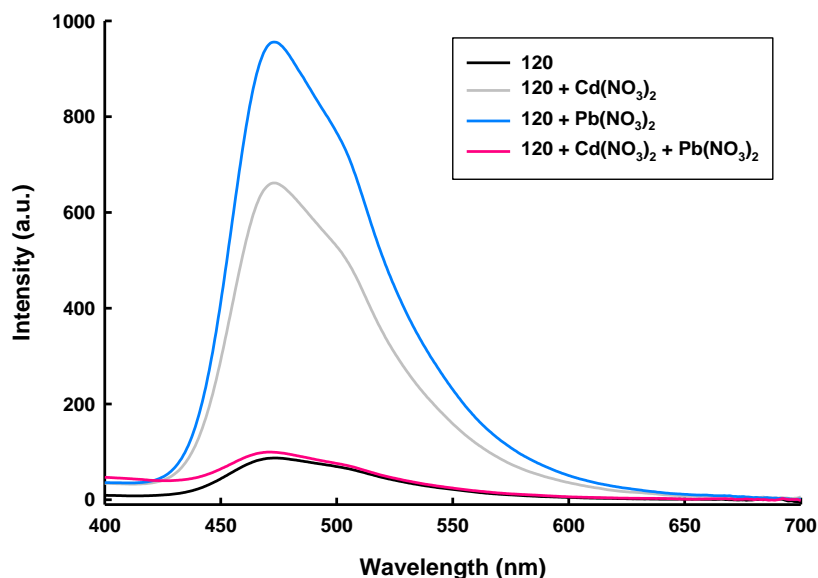


Figure 9. Fluorescence spectra of cyclophane **120** in presence of  $\text{Cd}(\text{NO}_3)_2$ ,  $\text{Pb}(\text{NO}_3)_2$  and the mixture of salts [(s):  $\sim 1.65 \times 10^{-6}$  M in DMF]

The complexation of cyclophane **120** presented in figure 9 behaves accordingly to the XOR logical operation (Table 8).

Table 8. Table of true for the XOR logic gate possible with **120**

Input 1	Input 2	Output
$\text{Cd}^{2+}$	$\text{Pb}^{2+}$	Fluorescence
0	1	1
1	0	1
1	1	0

The switching displayed by **120** is of importance for the development of new cyclophanes as switches and logic gates.

### II.3.4. Cyclic voltammograms of cyclophanes **119** and **120**

Electrochemical measurements were achieved for cyclophanes **119** and **120** in a conventional three electrodes system providing information about the redox properties of these new synthesized cyclophanes.

Cyclic voltammograms of cyclophanes **119** and **120** in the presence of some ions are depicted in figure 10 and the results are summarized in table 9.

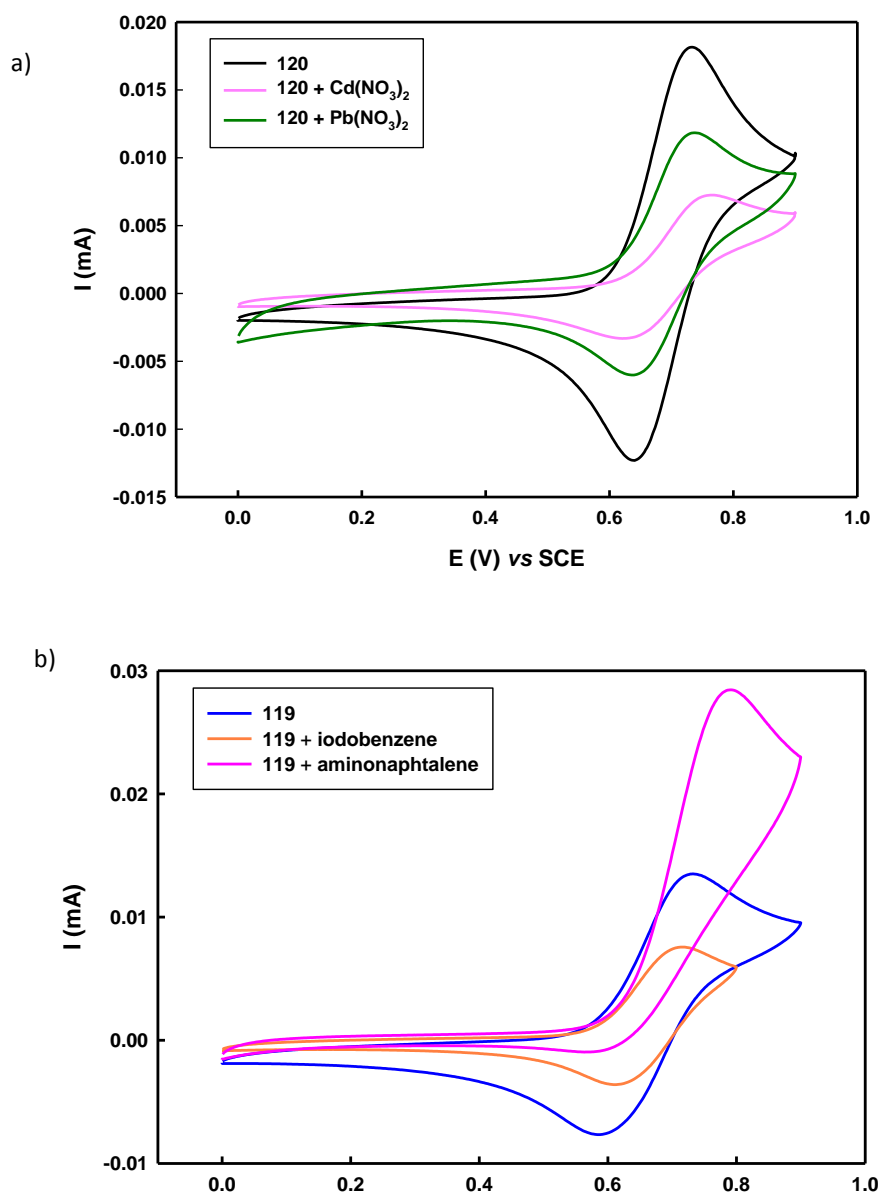


Figure 10. Cyclic voltammograms of cyclophanes **119** (a) and **120** (b) in DMF at *r.t.*; supporting electrolyte:  ${}^t\text{Bu}_4\text{N}^+\text{PF}_6^-$ ;  $\nu = 100$  mV/s, Pt working electrode, SCE reference electrode and Pt wire counter-electrode.

The electrochemical behavior in the presence of different cations doesn't produce significant changes in the redox behavior of cyclophanes, only a decreasing of the current from  $\text{Cd}^{2+}$  to  $\text{Pb}^{2+}$  (Figure 10 a) is noticed. In the system with organic molecules as guests the redox potential of **119** in presence of iodobenzene decreases as compared to cyclophane **119** and increases in the case of **119** with aminonaphthalene (Figure 10 b).

Table 9. Electrochemical data for the cyclophanes **119-120**

Samples	$\lambda_{\max}$ (s) [nm]	$\Delta E$ [eV]	$E_{pa}$ [mV]
<b>119</b>	280	4.43	732
<b>120</b>	280	4.43	734
<b>119 + iodobenzene</b>	268	4.63	715
<b>119+aminonaphthalene</b>	278	4.46	790
<b>120 + Cd(NO<sub>3</sub>)<sub>2</sub></b>	280	4.43	765
<b>120 + Pb(NO<sub>3</sub>)<sub>2</sub></b>	280	4.43	735

## II.4 Synthesis of new macrocycles with phenothiazine motifs applying dynamic constitutional chemistry principles

### II.4.1. Introduction

Constitutional Dynamic Chemistry (CDC) is a key method in organic synthesis. DCC make use of reversible chemical reactions which are running under thermodynamic control with the formation of a dynamic constitutional library (DCL) of compounds which are in equilibrium. The equilibrium ratios can be changed with the dramatic enhancement of the ratio (amplification) of one of the components of the library when a favored compound is largely stabilized (in many cases by interactions with a guest *via* supramolecular contacts) and due to this stabilization, the equilibrium is shifted towards this component (at the expense of other compounds of the library) and is obtained (after the freezing of the equilibrium) as major or exclusive product. The compounds of DCL reveal a continuous change in constitution by incorporation, reorganization, and exchange of building blocks<sup>7</sup> and the DCL shows a continuous modification till equilibrium is reached.

CDC opens novel perspectives in three main research areas<sup>8</sup>

- i) Supramolecular chemistry<sup>9</sup>—identification of dynamic receptors or substrates,
- ii) Biochemistry<sup>10</sup>.
- iii) Material sciences<sup>11</sup>-development of dynamic materials

<sup>7</sup>Lehn, J.-M. *Top. Curr. Chem.* **2012**, 322, 1-32

<sup>8</sup>Matache, M., Bogdan, E., Hädade, N. D. *Chem. Eur. J.* **2014**, 20, 2016-2131

<sup>9</sup>a) Furlan, R. L. E., Otto, S., Sanders, J. K. M. *Proc. Natl. Acad. Sci. USA* **2002**, 99, 4801–4804; b) de Bruin, B., Hauwert, P., Reek, J. N. H. *Angew. Chem.* **2006**, 118, 2726–2729; *Angew. Chem. Int. Ed.* **2006**, 45, 2660–2663; c) Otto, S., Severin, K. *Top. Curr. Chem.* **2007**, 277, 267–288; d) Otto, S. *J. Mater. Chem.* **2005**, 15, 3357–3361; e) Otto, S. *Curr. Opin. Drug Discov. Dev.* **2003**, 6, 509–520

<sup>10</sup>a) Sakulsombat, M., Zhang, Y., Ramström, O. *Top. Curr. Chem.* **2012**, 322, 55–86; b) Herrmann, A. *Org. Biomol. Chem.* **2009**, 7, 3195–3204; c) Lehn, J.-M., Eliseev, A. V. *Science* **2001**, 291, 2331–2332; d) Ramström, O., Lehn, J.-M. *Nat Rev Drug Discov.* **2002**, 1, 26–36; e) Miller, B. L. *Top. Curr. Chem.* **2012**, 322, 107–138.

<sup>11</sup>a) Mahon, E., Aastrup, T., Barboiu, M. *Top. Curr. Chem.* **2012**, 322, 139–164; b) Moulin, D. E., Cormos, G.; Giuseppone, N. *Chem. Soc. Rev.* **2012**, 41, 1031–1049; c) Lehn, J.-M. *Aust. J. Chem.* **2010**, 63, 611–623



In DLs (dynamic libraries), the interactions between building blocks may be covalent (Dynamic Combinatorial Libraries or Dynamic Covalent Libraries, DCL) or non-covalent (Dynamic Non-Covalent Libraries, DNCL). The composition of a DL is dependent on the environment, the internal properties of the product(s) (self-selection, self-assembly) or the interaction with external entities (e. g. template molecule, physical stimuli, or phase change) which may result in the amplification towards of a given type of compound (Figure 11)

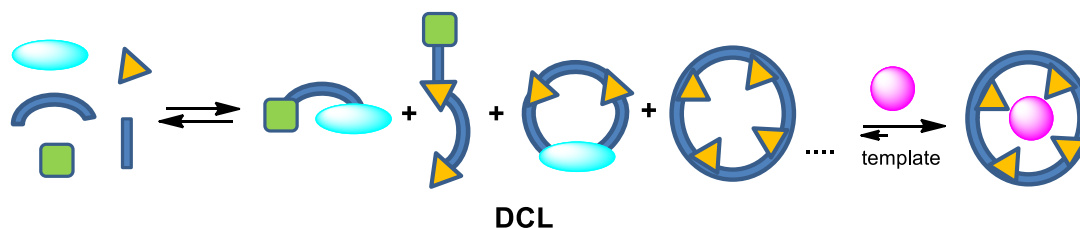


Figure 11. Schematic representation of the formation and evolution of a CDL in the presence of a template

The addition of a template shifts the equilibrium by forming favorable non-covalent interactions with one or more library members.<sup>9</sup> According to Le Châtelier principle the library recognizes to the new global energy minimum and adjusts composition to reach it.

In recent years chemists have exploited many reversible interactions in CDC. The most used for CDC are imine exchange,<sup>12</sup> which exhibits double dynamic processes<sup>7</sup>:

- i) configurational dynamics, - *cis-trans* isomerizations (photochemical and thermal)
- ii) constitutional dynamics, - exchange of the amine or/and carbonyl components<sup>13</sup>

#### II.4.2. Constitutional Dynamic Systems with 10*H*-phenothiazine dialdehydes and bis(aminomethyl)benzenes.

In this work we targeted to investigate the dynamic libraries and the possible amplifications resulted in the imine formation reactions of dialdehydes **101** and **102** (with phenothiazine units) with *ortho*-bis(aminomethyl)benzene **137** and *meta*-bis(aminomethyl)benzene **138** (Chart 4). The reactions of diamine **138** with dialdehydes **101** and **102** and of diamine **137** with dialdehyde **102** were experimented.

<sup>12</sup>a) Huc, I., Lehn, J. -M. *Proc. Natl. Acad. Sci. USA* **1997**, *94*, 2106-2110; b) Cantrill, S. J., Rowan, S. J., Stoddart, J. F. *Org. Lett.* **1999**, *1*, 1363-1366; c) Oh, K., Jeong, K. S., Moore, J. S. *Nature* **2001**, *414*, 889-893; d) Storm, O. Lüning, U. *Chem. Eur. J.* **2002**, *8*, 793-798; e) Chichak, K. S., Cantrill, S. J., Pease, A. R., Chiu, S.-H., Cave, G. W. V., Atwood, J. L., Stoddart, J. F. *Science* **2004**, *304*, 1308-1312

<sup>13</sup>Lehn, J.-M. *Chem. Eur. J.* **2006**, *12*, 5910-5915

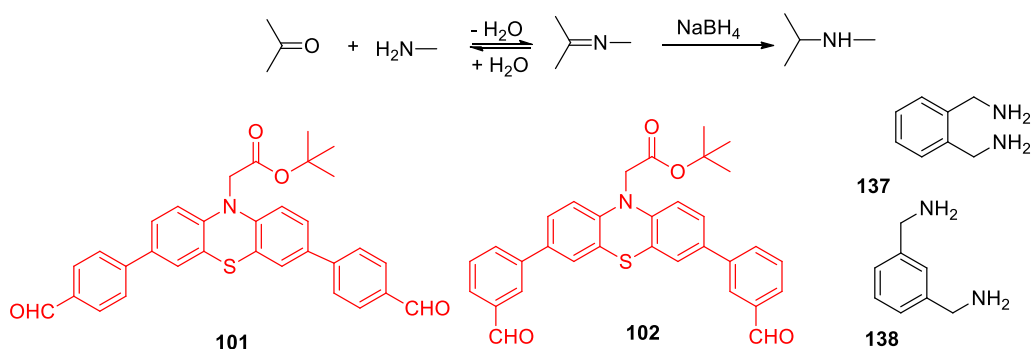
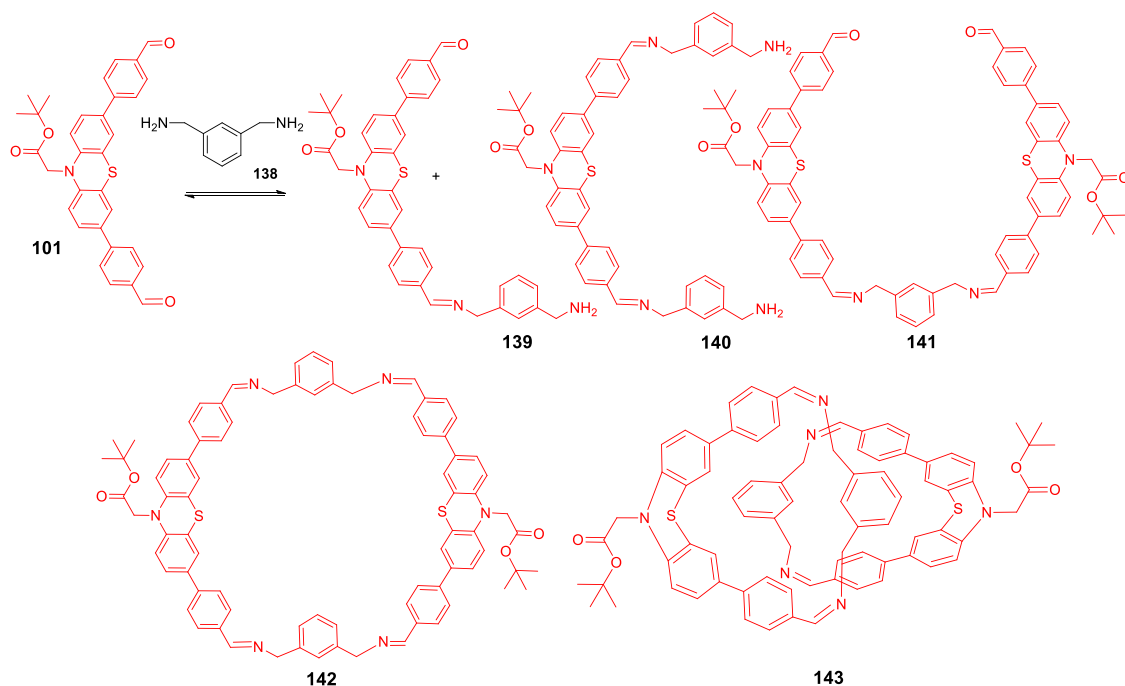


Chart 4. Building blocks for providing imine libraries

The imine formation reactions were carried out in anhydrous dichloromethane, at reflux, under argon. In all cases, at different moments (one, three and six hours; one, two, five and six days) samples of the reaction mixtures were collected and the reactions were frozen by cooling and immediate reduction of the crude products with  $\text{NaBH}_4$  when the imine groups were transformed into amines and the further chemical equilibrations were avoided.

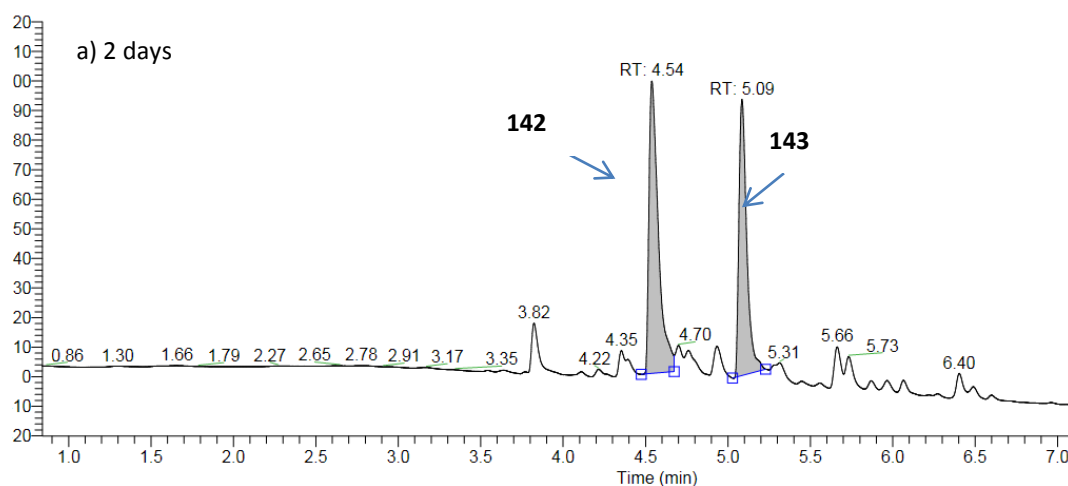
In all investigated cases the thermodynamic equilibrium was reached after six days of monitoring the reactions (in several experiments, the reactions were monitored for longer periods and no significant changes were observed after the sixth day).

In the case of the reaction of dialdehyde **101** and diamine **138** (Scheme 18) the first chromatograms (after 3 and 6h) showed the formation of the monoimine **139** ( $R_t = 4.59$ ;  $m/z = 644$ , 65%) and of the diimine **140** ( $R_t = 4.66$ ;  $m/z = 759$ , 15%) together with the appearance of a compound with  $m/z = 1252$  ( $R_t = 4.57$  min; 20 %). The chromatogram recorded after 1 day exhibits as major product (90%) the compound with  $R_t = 4.57$  min. The MS measurements (after reduction of the sample with  $\text{NaBH}_4$ ) revealed for this peak the presence of the monocharged ion with  $m/z = 1252$  and the dicharged ion at  $m/z = 626$ . These  $m/z$  values can be associated either to the catenane **143** or to the isomeric macrocycle **142** as members of DCL.



Scheme 18. Components of the imines library generated by dialdehyde **101** and diamine **138**

The chromatogram after 2 days (Figure 12a) shows a considerable diminishing of the intensities of the peaks corresponding to the acyclic compounds and the formation of a second compound ( $R_t = 5.09$  min) with the same  $m/z = 1252$  value. The two peaks with  $m/z = 1252$  are the major components (about 50% and 50%), and they correspond to the reduced forms of isomeric macrocycle **142** and catenane **143**. Finally, at equilibrium (after 6 days) the major product ( $\approx 90\%$ ) corresponds to the compound at  $R_t = 4.57$  min. (Figure 12b) and it is either the macrocycle or the catenane which generate the peak  $m/z = 1252$  in the sample.



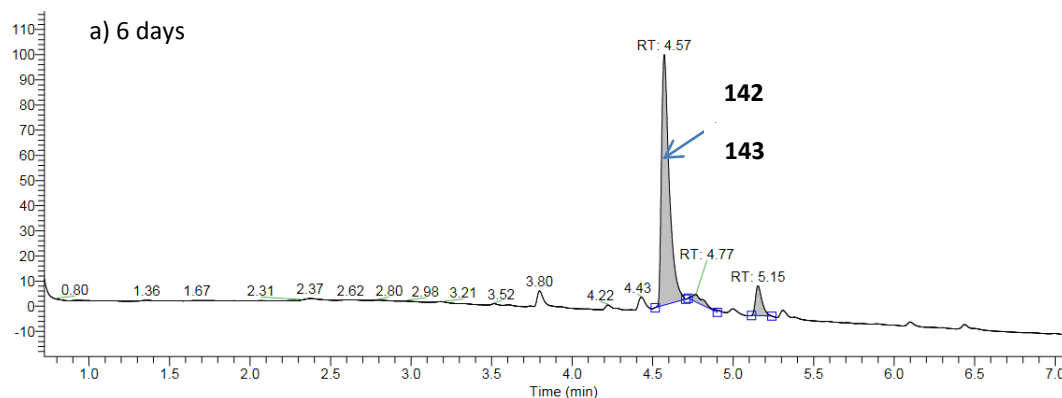


Figure 12. HPLC-MS analysis of the members of library at 2 (a) and 6 days (b)

The final  $m/z = 1252$  product was separated using semipreparative HPLC ( $C_{18}$ , 30%-70% water(containing 0.1% TFA) /acetonitrile as gradient, with a flow rate of  $5 \text{ mL min}^{-1}$ , and UV detection at 230, 254 and 280 nm).  $^1\text{H}$  NMR spectrum of this compound is given in figure 13.

The recorded signals correspond to the proposed structures (macrocycle or catenane) but an assignment of the spectrum to one of these structures was not possible. The spectrum exhibits a singlet for the protons of the *t*-butyl groups ( $\delta = 1.53 \text{ ppm}$ ), three singlets ( $\delta = 4.25, 4.28$  and  $4.53 \text{ ppm}$ ; ratios of intensities = 2/2/1) corresponding to the methylene units either connecting the amino groups or belonging to the *N*-methylester groups, respectively. Some of the signals of the aromatic protons are fitting to the phenothiazine units give the specific pattern [ $\delta = 6.74$  (doublet, 1-H, 9-H);  $7.32$  (doublet, 4-H, 6-H);  $7.39 \text{ ppm}$  (doublet of doublets, 2-H, 8-H)], while the other aromatic protons give groups of overlapped peaks and their assignment was not possible.

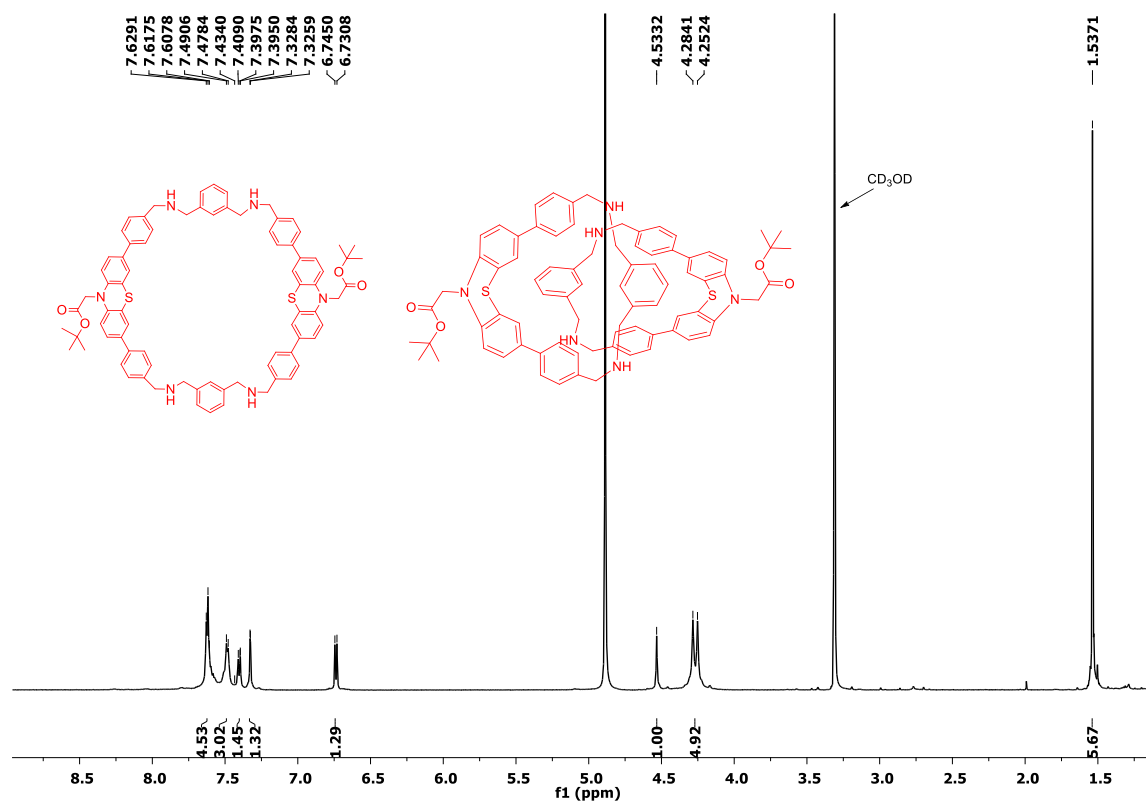


Figure 13.  $^1\text{H}$  NMR spectrum of the separated macrocyclic compound with  $R_t = 4.57$

## II. 5. Investigation of some protection and deprotection reactions

In this chapter some aspects concerning the protection and deprotection reactions for some functionalities encountered in our target compounds are discussed. One of the challenges that organic chemists have to solve is connected to the unwanted side reactions, occurred due to several functional groups present in the substrate. The byproducts make more difficult the isolation of the desired compounds and their formation diminish the yields of the target transformations. The solution accepted long time ago is the protection of the groups which have to be preserved during the reaction. The removal of the protecting groups at the end of the reactions has to be done in mild conditions, without the damaging of the other functional groups of the substrate.

Aldehydes and ketones are usually protected as cyclic acetals and ketals (1,3-dioxanes and 1,3-dioxolanes), because these cyclic compounds are stable in basic environments and can be easily removed in acidic conditions.

The protection as 1,3-dioxane derivatives is carried out with 1,3-propane diols.

A series of cryptands displaying 1,3-dioxane moieties (protected carbonyl groups) in the main structural unit were synthesized in our group (Chart 5).<sup>14</sup>

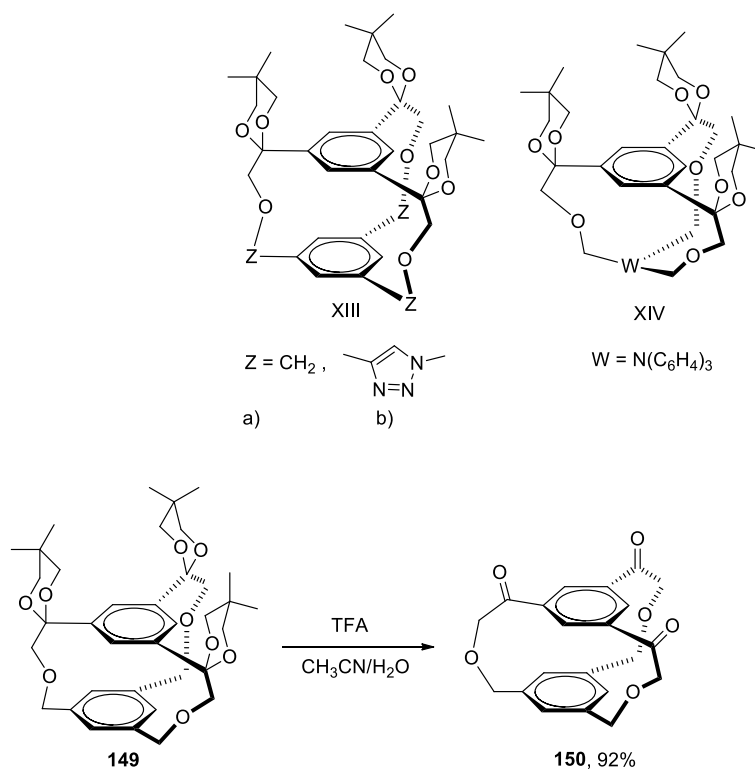


Chart 5. Cryptands (XIII and XIV) exhibiting protected carbonyl groups<sup>14</sup>

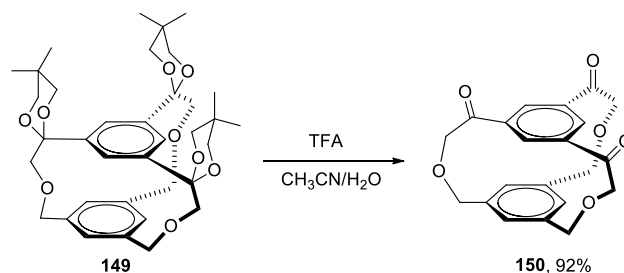
For the deprotection of the cryptand **149** (Chart 5, XIII, Z = CH<sub>2</sub>; Scheme 19) several conditions (shown in table 10) based either on the CAN and HCl or on trifluoroacetic acid (TFA) deprotection systems were investigated.

The previously reported methods (as shown in Table 10) were unsuccessful and only the deprotection with trifluoroacetic acid (TFA) in acetonitrile/water as solvents gave very good yields (92%; scheme 50). The total deprotection was confirmed by the <sup>1</sup>H NMR spectrum of **150** (Figure 14).

Table 10. Results of the deprotection experiments run with XIII a

Solvents	Deprotection systems	Temperature (°C)	Results
CH <sub>3</sub> CN/H <sub>2</sub> O	CAN/HCl	20, 60	Mixture of partially deprotected cryptands
DCM/H <sub>2</sub> O	TFA	20, 40	Mixture of partially deprotected cryptands
DCM/ H <sub>2</sub> O	CAN/TFA	20	Mixture of partially deprotected cryptands
CH <sub>3</sub> CN/H <sub>2</sub> O	TFA	50	Total deprotection Yields 92%

<sup>14</sup> Cîrcu, M., Soran, A., Hädade, N. D., **Rednic, M.**, Terec, A., Grosu, I. *J. Org. Chem.* **2013**, 78, 8722-8729



Scheme 19. Deprotection reaction of **149** in the presence of TFA

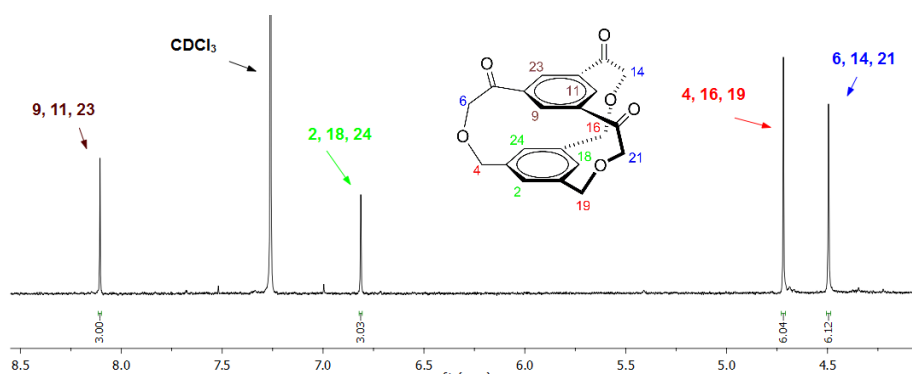


Figure 14.  $^1\text{H}$  NMR spectrum (fragment) of compound **150** (represented from reference 57)

### III. Conclusions

A detailed literature survey concerning macrocyclic compounds exhibiting phenothiazine or other heterocycles as acridine, acridane or phenazine was performed.

Phenothiazine based dipodands decorated with reactive groups at positions 3,7 and 10 (in several cases) were obtained in good yields and were further used for the synthesis of macrocyclic compounds

Four cyclophanes and one cryptand exhibiting two or three phenothiazine based bridges were obtained in fair or good yields using a strategy which involves aromatic nucleophilic substitution reactions. The absorption and emission spectra of these macrocycles revealed spectacular modifications when cations, anions or organic molecules were used as guests. For a system formed by two cations and cyclophane the modifications of the emission spectra allowed the building of a XOR molecular logical gate.

Constitutional dynamic libraries were obtained using phenothiazine based dialdehydes and bis(methylamino)benzenes. The HPLC-MS investigations of these dynamic libraries pointed out the evolution of the system towards macrocyclic compounds which became after six days the major products. The identity of these macrocycles could not be univocally determined, a dimer macrocycle and a catenane being possible accordingly to the molecular weight and the  $^1\text{H}$  NMR of the final compound.

An efficient method for the triple deprotection of a cryptand decorated with three 1,3-dioxane units was elaborated.

## Part B. Anion sensing via $\beta$ -HCH complexes

### I.1. Introduction

Supramolecular chemistry, defined by Jean-Marie Lehn as the chemistry “beyond the molecules”, or as the chemistry of secondary (intermolecular) interactions, is investigating the architectures built with host and guest molecules. The hosts are in many cases macrocyclic compounds, while the guests are cations, anions or neutral molecules<sup>15,16,17</sup>

These works mainly focused on the investigation of the complexes formed by sophisticated macrocyclic compounds and atomic or molecular anions. Many macrocycles (e. g. crown ethers, resorcinol or pillar arenes)<sup>18</sup>, cryptands,<sup>19</sup> rotaxanes<sup>20</sup> or catenanes<sup>21</sup> revealed the ability to complex different anions (with a preference for sturdier halide ones).

In 1968, at Babes-Bolyai University, prof. Sorin Mager<sup>22</sup> elaborated an ingenious method to quantitatively separate  $\beta$ -HCH from the mixture of isomers (formed in the chlorination reaction of benzene, Chart 6) *via* its crystalization with PyxHCl or PyxHBr. These molecular complexes could be separated by filtration.  $\beta$ -HCH forms complexes with other heterocyclic salts (such as: hydrochlorides and hydrobromides of  $\beta$ - and  $\gamma$ -picolines, 2,4,6-collidine, 2,2'-bipyridine, isoquinoline and acridine).<sup>23</sup> The authors took into consideration interactions between the chlorine atoms of  $\beta$ -HCH in a

---

<sup>15</sup>a) Steed, J. W., Atwood, J. L., *Supramolecular Chemistry*, Wiley & Sons, New-York, **2009**; b) Davis, F., Higson, S. *Macrocycles: Construction, Chemistry and Nanotechnology Applications*, Wiley & Sons, New York, **2011**; c) Lee, M. H., Kim, J. S., Sessler, J. L. **Chem. Soc. Rev.** **2015**, **44**, 4185-4191; d) Langton, M. J., Beer, P. D. *Acc. Chem. Res.* **2014**, **47**, 1935–1949; e) He, Q., Zhang, Z., Brewster, J. T., Lynch, V. M., Kim, S. K., Sessler, J. L. *J. Am. Chem. Soc.* **2016**, **138**, 9779–9782

<sup>16</sup> Evans, N. H. Beer, P. D. *Angew. Chem. Int. Ed.* **2014**, **53**, 11716 – 11754; b) Gale, P. A., Caltagirone, *Chem. Soc. Rev.*, **2015**, **44**, 4212-4227; c) Frontera, A., Gamez, P., Mascial, M., Mooibroek, T. J., Reedijk, J. *Angew. Chem. Int. Ed.* **2011**, **50**, 9564 – 9583; d) Dutta, R., Ghosh, P. *Chem. Commun.* **2015**, **51**, 9070 – 9084; e) Zhang, Z., Kim, D. S. Lin, C.-Y., Zhang, H., Lammer, A. D., Lynch, V. M., Popov, I. Miljanić, O. Š., Anslyn, E. V., Sessler, J. L. *J. Am. Chem. Soc.* **2015**, **137**, 7769–7774,

<sup>17</sup>Barnes, J. C., Juriček, M., Strutt, N. L., Frascioni, M., Sampath, S., Giesener, M. A., McGrier, P. L., Burns, C. J., Stern, C. L., Sarjeant, A. A., Stoddart, J. F., *J. Am. Chem. Soc.* **2013**, **135**, 183-192; b) Chi, X., Zhang, H., Vargas-Zúñiga, G. I., Peters, G. M., Sessler, J. L. *J. Am. Chem. Soc.* **2016**, **138**, 5829–5832,

<sup>18</sup>a) Howe, E. N. W, Bhadbhade, M., Thordarson, P. *J. Am. Chem. Soc.* **2014**, **136**, 7505–7516; b) Mullaney, B. R., Thompson, A. L., Beer, P. D. *Angew. Chem. Int. Ed.* **2014**, **53**, 11458 –11462; c) Yu, G., Zhang, Z., Han, C., Xue, M., Zhou, Q. Huang, F. *Chem. Commun.* **2012**, **48**, 2958–2960

<sup>19</sup>Perraud, O., Robert, V., Gornitzka, H., Martinez, A., Dutasta, J.-P. *Angew. Chem. Int. Ed.* **2012**, **51**, 504 -508

<sup>20</sup>a) Allain, C., Beer P. D., Faulkner, S., Jones, M. W., Kenwright A. M., Kilah, N. L., Knighton, R. C., Sørensen, T. J., Tropiano, M. *Chem. Sci.*, **2013**, **4**, 489-493; b) Mercurio, J. M., Knighton, R. C., Cookson, J., Beer, P. D. *Chem. Eur. J.* **2014**, **20**, 11740 – 11749; c) White, N. G., Costa, P. J., Carvalho, S., Félix, V., Beer, P. D. *Chem. Eur. J.* **2013**, **19**, 17751 – 17765

<sup>21</sup>a) Langton, M. J., Beer, P. D., *Chem. Commun.* **2014**, **50**, 8124 – 8127; b) Gil-Ramírez, G., Leigh, D. A. Stephens, A. J. *Angew. Chem. Int. Ed.* **2015**, **54**, 6110 – 6150

<sup>22</sup>Mager, S., Ionescu, M. *Stud. Univ. Babeş-Bolyai, Chem.* **1968**, **2**, 107-110,

<sup>23</sup>a) Ionescu, M., Mager, S. *Rev. Roum. Chim.* **1968**, **13**, 631-636; b) Mager, S., Horn, M., Hopârtean, I., Motiu, A. *Monatsh. Chem.* **1978**, **109**, 1403-1412



conformation with all chlorine atoms in axial orientations and the aromatic cations of the salts as a driving force in the formation of these complexes. In the context of the high interest for anions detection and of the similarity of the stereochemistry of 1,3,5-trioxane of Cho's work<sup>24</sup> and of the *all-cis* isomer of hexafluorocyclohexane of McMahon's work<sup>25</sup> to that of  $\beta$ -HCH (Chart 7) we decided to revisit  $\beta$ -HCH complexes reported by Mager<sup>12</sup> using both pyridinium and tetrabutylammonium salts and to investigate the interactions of  $\beta$ -HCH with several anions<sup>26</sup>

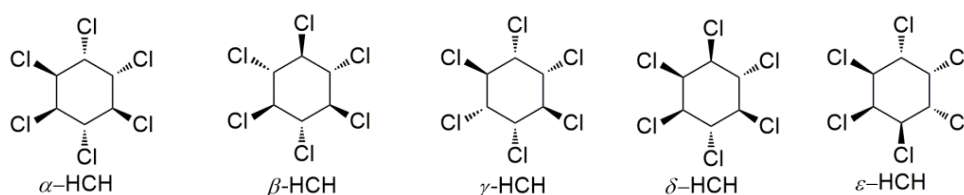


Chart 6. Diastereoisomers of HCH

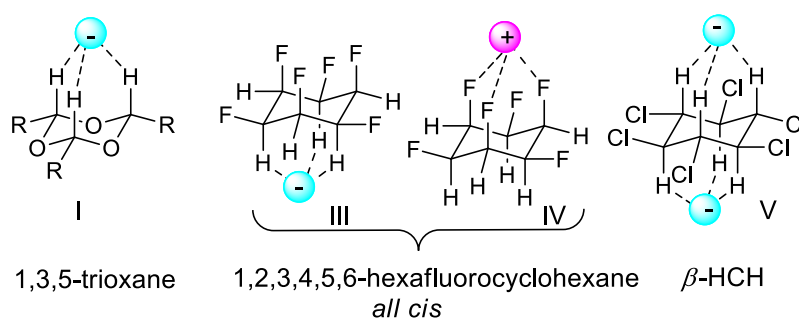


Chart 7. Illustration of the anion-1,3,5-trioxane (I), of the peculiar complexation of *all-cis* hexafluorocyclohexane (III, IV) and of the expected contacts in anion- $\beta$ -HCH complexes (V)

## II. Interactions of $\beta$ -HCH with $\text{Cl}^-$ , $\text{Br}^-$ , $\text{I}^-$ and $\text{HSO}_4^-$

### II.1. Solid state investigations

Single crystals suitable for X ray diffraction measurements could be obtained using  $\beta$ -HCH and PyxHCl (crystallization from chloroform) PyxHBr (crystallization from pyridine) and for  $\beta$ -HCH itself (6).

<sup>24</sup>Shi, G., Gadhe, C. G., Park, S.-W., Kim, K. S., Kang, J., Seema, H., Singh, N. J., Cho, S. J. *Org. Lett.*, **2014**, *16*, 334-337

<sup>25</sup>Ziegler, B. E., Lecours, M., Marta, R. A., Featherstone, J., Fillion, E., Hopkins, W. S., Steinmetz, V. Keddie, N. S., O'Hagan, D., McMahon, T. B. *J. Am. Chem. Soc.* **2016**, *138*, 7460-7463

<sup>26</sup>**Rednic, M. I.**, Varga, R. A., Bende, A., Grosu, I. G., Miclăuş, M., Hădade, N. D., Terec, A., Bogdan, Elena Grosu, I. **2016** submitted

$\beta$ -HCH (1) crystallizes in a high symmetry cubic form and its molecular structure shows a chair conformation exhibiting the chlorine atoms in equatorial orientations. In the lattice (Figure 15), bifurcated contacts for each chlorine atom of a molecule with H atoms of six different neighboring molecules are observed. The H atoms of the same molecule give similar contact with other six molecules situated on both sides of the central reference  $\beta$ -HCH unit. ( $d_1 = 3.046$  and  $d_2 = 3.080$  Å; C-Cl...H angles are  $\alpha_1 = 111.87$  and  $\alpha_2 = 113.08$  °). The elementary cell for the crystal structure of this compound is a cube.

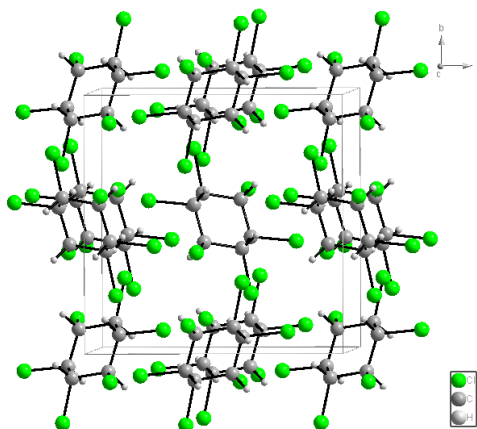


Figure 15. X-ray molecular structure of  $\beta$ -HCH: representation of the lattice (reproduced from reference 26)

The following molecular combinations between  $\beta$ -HCH and these salts were obtained:  $C_6H_6Cl_6 \times 2C_5H_5N^+ - Hx2Cl^-$  (**7**),  $C_6H_6Cl_6 \times 2C_5H_5N^+ - Hx2Br^-$  (**8**),  $C_6H_6Cl_6 \times C_5H_5NxC_5H_5N^+ - HxBr^-$  (**9**). The relevant units (Figure 16) show for **7** and **8** (these structures are similar) two anions on the  $C_3$  axis of  $\beta$ -HCH (one on the top and the other at the bottom of the reference plane of  $\beta$ -HCH). Each  $\beta$ -HCH displays six axial CH/ $X^-$  short contacts ( $d_{Cl(-) \cdots HC(sp^3)} = 2.866, 2.866$  and  $2.710$  Å for **7**;  $d_{Br(-) \cdots HC(sp^3)} = 2.965, 2.965$  and  $2.847$  Å for **8**). In addition in the lattices (Figures 17 and 18) each anion ( $Cl^-$  or  $Br^-$ ) shows contacts with three pyridinium units: a  $N^+ - H \cdots X^-$  interaction ( $d_{Cl(-) \cdots H-N(+)} = 2.102$ ;  $d_{Br(-) \cdots H-N(+)} = 2.294$  Å) and two identical  $C(sp^2) - H \cdots X^-$  contacts ( $d_{Cl(-) \cdots H-C(sp^2)} = 2.645$ ;  $d_{Br(-) \cdots H-C(sp^2)} = 2.823$  Å). In **7** and **8** each pyridinium moiety is connected to three anions.

The pyridine rings connected by  $X^- \cdots H-C(sp^2)$  contacts generate chains with alternating pyridine-anion units. All pyridine units in a chain are coplanar and the  $N$  atoms are oriented on the same side. Two neighbouring chains have parallel pyridine rings that are placed in slightly distanced planes (about  $0.8$  Å in **7** and **8**) and show antiparallel orientations of  $N$  atoms. These chains are connected to each other, generating ribbons with a  $\beta$ -sheet profile *via*  $N^+ - H \cdots X^-$  contacts (Figure 16

and 17). These parallel ribbons are connected to each other by  $\beta$ -HCH units *via* the six  $X^- \cdots H-C(sp^3)$  contacts generating a 2D network. In the lattices of both **7** and **8**, each pyridine ring has an additional bifurcated  $C(sp^2)-H \cdots Cl-C(sp^3)$  contact (**7**:  $d_{Cl \cdots H-C} = 2.949 \text{ \AA}$  and **8**:  $d_{Cl \cdots H-C} = 2.972 \text{ \AA}$ ) involving the  $C(sp^2)-H$  bond at position 4 and two neighbouring  $\beta$ -HCH molecules belonging to other 2D entity (Figures 17 and 18). These contacts ensure the 3D structure of the lattice.

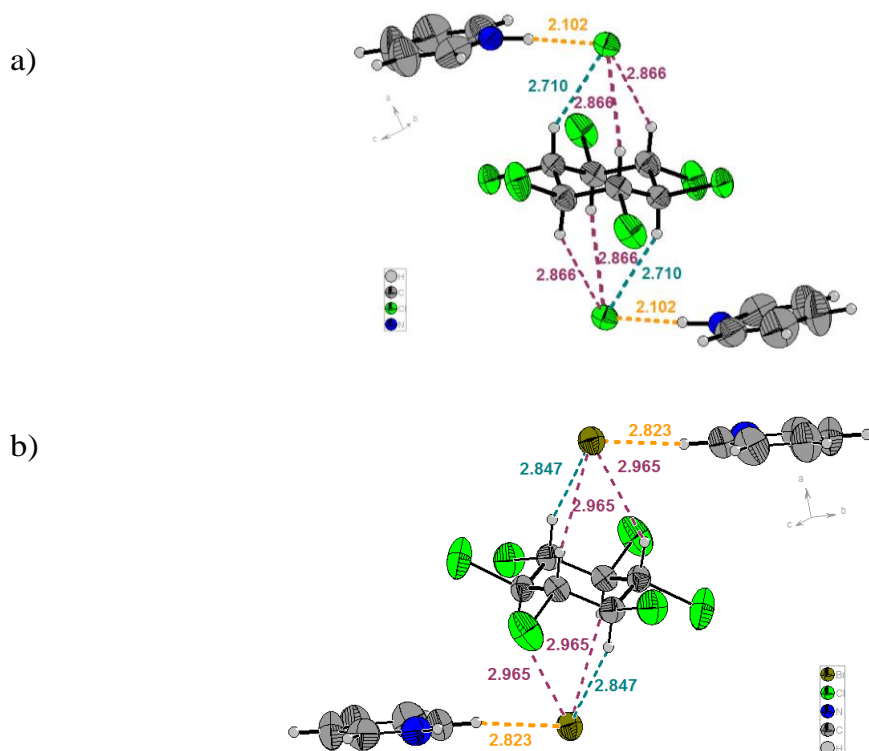


Figure 16. Representations of typical repetitive units for **7** (a) and **8** (b)

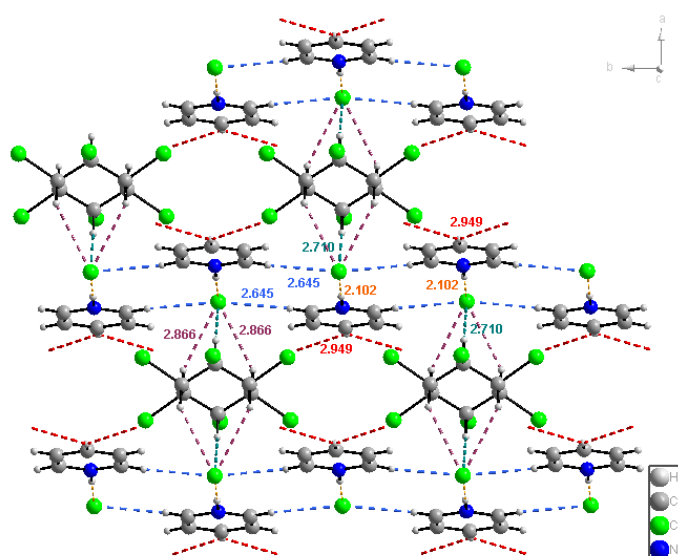


Figure 17. Representation of solid state supramolecular network of **7** [the  $\beta$ -sheet type ribbons (contact in orange and blue) and the 2D structure are shown in detail, while the formation of the 3D aggregate is

suggested by the contacts (in red) involving the H atom at position 4 of pyridine units]

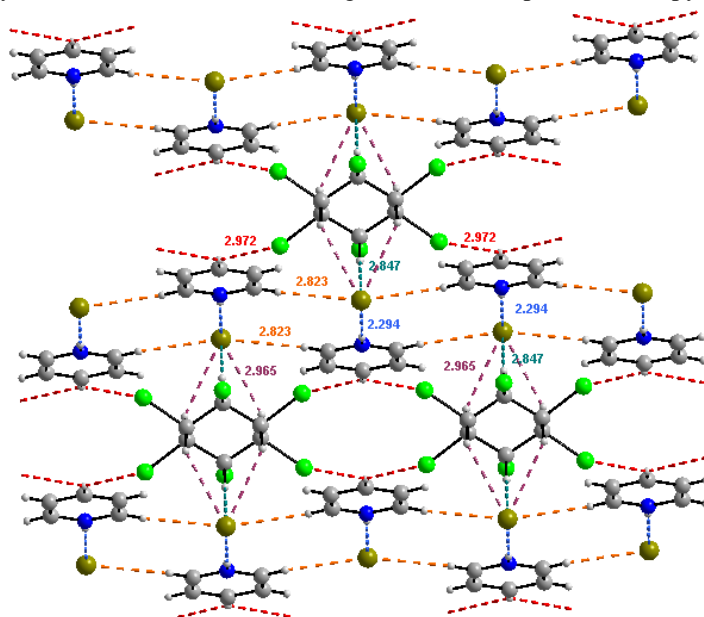


Figure 18. Representation of solid state supramolecular network of **8** [the  $\beta$ -sheet type ribbons (contact in orange and blue) and the 2D structure are shown in detail, while the formation of the 3D aggregate is suggested by the contacts (in red) involving the H atom at position 4 of pyridine units]

In the case of **9**, two pyridine rings are connected to each other and share a proton ( $H^+$ ), the distance between the *N* atoms of the heterocycles being only 2.696 Å.

In the lattice of **9** (Figures 19 and 20)  $\beta$ -HCH and  $Br^-$  form spectacular columns built by six  $C(sp^3)-H \cdots Br^-$  contacts/molecule. The columns are connected to each other by halogen bonding  $C(sp^3)-Cl \cdots Cl-C(sp^3)$  ( $d = 3.451$  Å) and form a 2D sheet. Each bromide anion has two  $C(sp^2)-H \cdots Br^-$  contacts with H atoms at positions 2 and 4, of pyridinium rings from two different pyridinium-pyridine units, respectively ( $d_{Br(-) \cdots H-C(sp^2)} = 2.927$  and  $2.969$  Å). These contacts connect columns of different sheets and determine the 3D structure of the supramolecular polymer (Figure 20).

An illustrative representation is shown in figure 21, where the arrangements of  $\beta$ -HCH and  $Br^-$  anions are compared to the infinity column of Brâncuși.

In figure 22 the reference unit of **9** is shown in order to illustrate the  $C(sp^3)-H \cdots Br^-$  contacts, the pyridinium-pyridine interaction and the  $C(sp^2)-H \cdots$  anion bonds as well as the interactions involved in the connection of two adjacent columns.

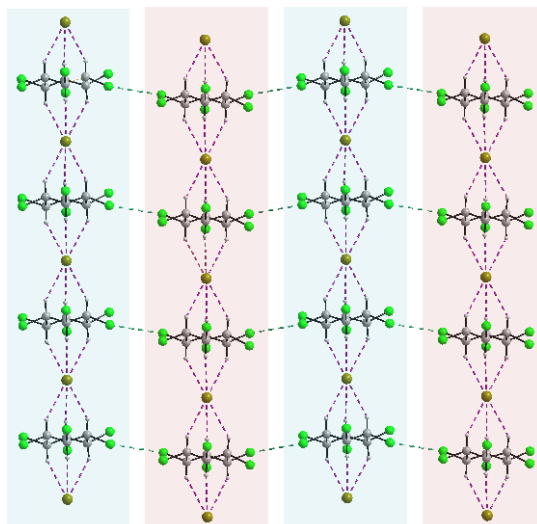


Figure 19. Representation of solid state supramolecular 2D network of **9**. Reproduced from reference 26

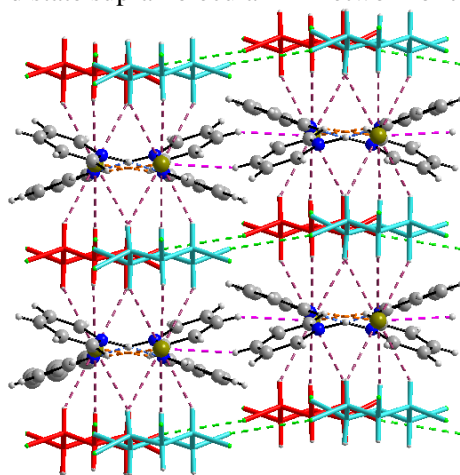


Figure 20. Representation of solid state supramolecular 3D network of **9** by the participation of the pyridinium-pyridine units. Reproduced from reference 26

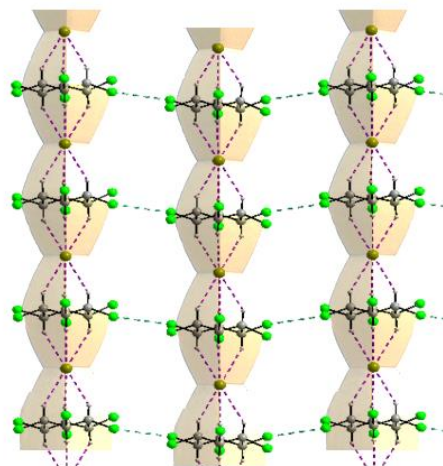


Figure 21. Comparison of the 1D structure of **9** with the infinity column of Brâncuși. Reproduced from reference 26

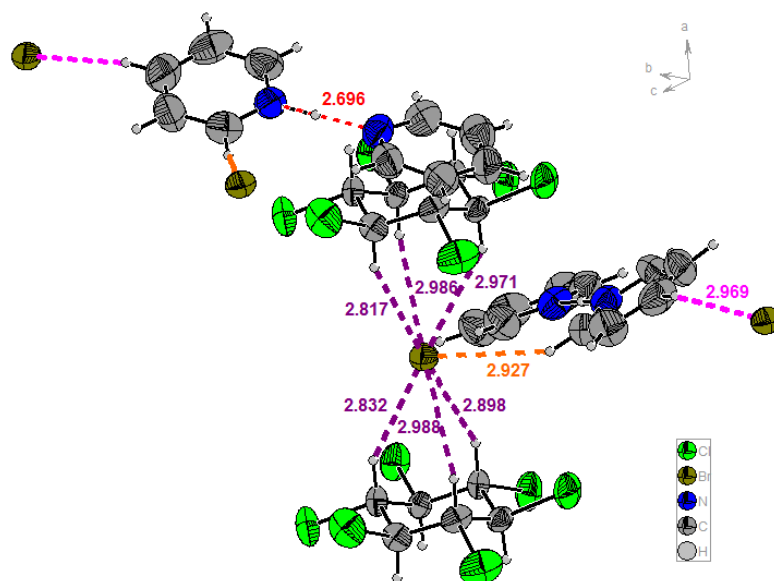


Figure 22. Representation of a typical repetitive unit in the crystal structure of **9**. Reproduced from reference 26

## II.2. Investigations in solution

The stoichiometry of the host-guest complexes between  $\beta$ -HCH and different anions ( $\text{Cl}^-$ ,  $\text{Br}^-$ ,  $\text{I}^-$  and  $\text{HSO}_4^-$ ) was determined by  $^1\text{H}$  NMR titration at *r.t.* In each case nine NMR samples in various host/guest ratios (Table 1) were prepared using 5mM stock solutions of  $\beta$ -HCH (**6**, 5mM) in  $\text{CD}_3\text{CN}$  and salts exhibiting the target anions **A1** (pyridinium hydrochloride), **A2** (pyridinium hydrobromide), **A3** [tetrabutylammonium iodide (TBAI)] and **A4** [tetrabutylammonium hydrogensulfate (TBAHS)] at a final concentration of 5 mM (host [H] + guest [G]).

The changes in the chemical shifts of  $\beta$ -HCH signal at 4.2560 ppm with increasing amounts of guest are indicated for A1 in table 11 and the determination of the main experimental data in figures 23 and 24.

Since the binding equilibrium has a very fast exchange rate compared to the NMR time scale a modified Job plot<sup>27</sup> was used in order to determine the complex stoichiometry. Thus,  $\Delta\delta \times [\text{H}]$  was plotted as y-coordinate and  $[\text{H}] / ([\text{H}]+[\text{G}])$  as x-coordinate as shown in figures 23 and 24. The obtained data suggest in all cases the 1:1 binding stoichiometry.

a) Details of the JOB-PLOT experiment run with A1

<sup>27</sup>Hirose, K. *J. Incl. Phenom. Mol. Recognit. Chem.* **2001**, 39, 193-209

Table 11.  $^1\text{H}$  NMR titration data for guest A1

HCH $\mu\text{L}$	PyxHCl $\mu\text{L}$	nHCH $\text{mM} \times 10^3$	nPyxHCl $\text{mM} \times 10^3$	$[\text{HCH}] /$ $([\text{HCH}] + [\text{PyHCl}])$	$\Delta\delta$ ppm	$\Delta\delta \times$ nHCH	$\delta_{\text{exp}}$ ppm
50	450	0.25	2.25	0.1	0.0091	0.002275	4.2651
100	400	0.50	2.00	0.2	0.0084	0.0042	4.2644
150	350	0.75	1.75	0.3	0.0077	0.005775	4.2637
200	300	1.00	1.50	0.4	0.0066	0.0066	4.2626
250	250	1.25	1.25	0.5	0.0058	0.00725	4.2618
300	200	1.50	1.00	0.6	0.0047	0.00705	4.2607
350	150	1.75	0.75	0.7	0.0036	0.0063	4.2596
400	100	2.00	0.50	0.8	0.0022	0.0044	4.2582
450	50	2.25	0.25	0.9	0.0010	0.00225	4.2570

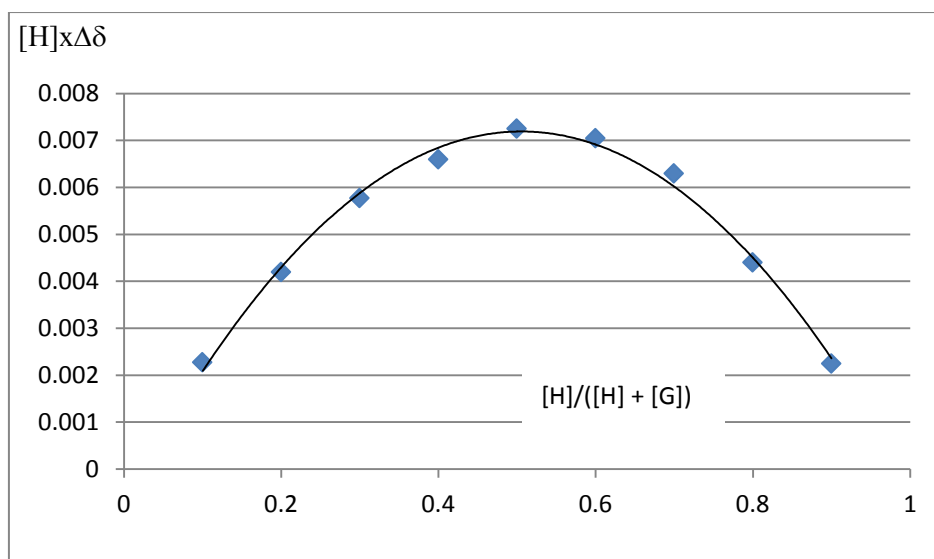


Figure 23. Job plot of **6** (5mM) with **A1** (5mM) in  $\text{CD}_3\text{CN}$

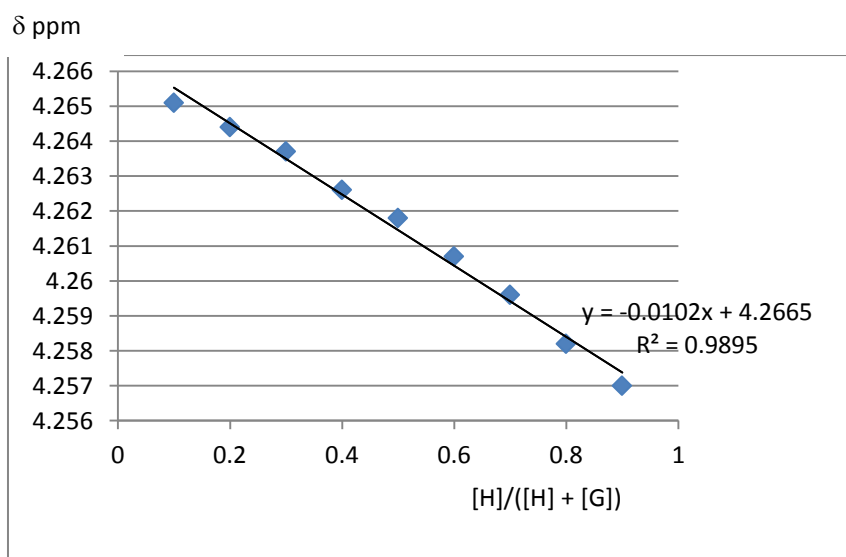


Figure 24. Determination of  $\delta_c$

The association constants (Table 12) were calculated using following equations:

$$\delta = \frac{[H] - x}{[H]} * \delta_H + \frac{x}{[H]} * \delta_C$$

$$K = \frac{x}{([G] - x)([H] - x)}$$

where [H] and [G] are the concentrations corresponding to the total amounts of host (H) and guest (G) and x is the concentration of the formed complex, while  $\delta$ ,  $\delta_H$  and  $\delta_C$  are the experimental  $\delta$  values of the test signal at different host/guest ratios ( $\delta$ ), the  $\delta$  value of the test signal in the free host molecule ( $\delta_H$ ) and the  $\delta$  value of the test signal in the complex ( $\delta_C$ ).

Table 12. Values of the association constants for A1-A4

Guest	$\delta_c$ ppm	K L/mol x 10 <sup>3</sup>			Average K value L/mol x 10 <sup>3</sup>
		[H]/[G] ratio			
		1/1.5	1/1	1.5/1	
PyxHCl	4.2665	1.94	2.20	2.46	2.20 ± 0.26
PyxHBr	4.3104	1.58	1.95	1.83	1.79 ± 0.19
TBAI	4.2823	1.78	1.56	1.70	1.68 ± 0.11
TBAHS	4.2665	1.36	1.62	1.07	1.35 ± 0.28

The  $\delta_c$  values were obtained from the linear representation  $\delta = f \{ [H]/([H]+[G]) \}$  (Figure 24). The K values were calculated for the H/G ratios 1/1.5; 1/1 and 1.5/1 giving the reported average values.

The affinity of  $\beta$ -HCH and for the investigated anions (Cl<sup>-</sup>, Br<sup>-</sup>, I<sup>-</sup> and HSO<sub>4</sub><sup>-</sup>) was also demonstrate by ESI(-)-HRMS experiments.

The ESI(-)-spectra of 5 mM solutions of HCM and pyridinium chloride, bromide, or tetrabutylammonium iodide and hydrogen sulfate, 1:9 molar ratio, in acetonitrile, shows characteristic peaks at  $m/z = 324.8267$ ,  $370.7728$ ,  $416.7618$  and  $386.8163$  corresponding to the monocharged species [HCH+Cl]<sup>-</sup>, [HCH+Br]<sup>-</sup>, [HCH+I]<sup>-</sup> and [HCH+HSO<sub>4</sub>]<sup>-</sup>, respectively suggesting the formation of 1:1 complexes in all cases. The ESI(-)-HRMS spectra for A2 and A4 are shown in figures 25-26.



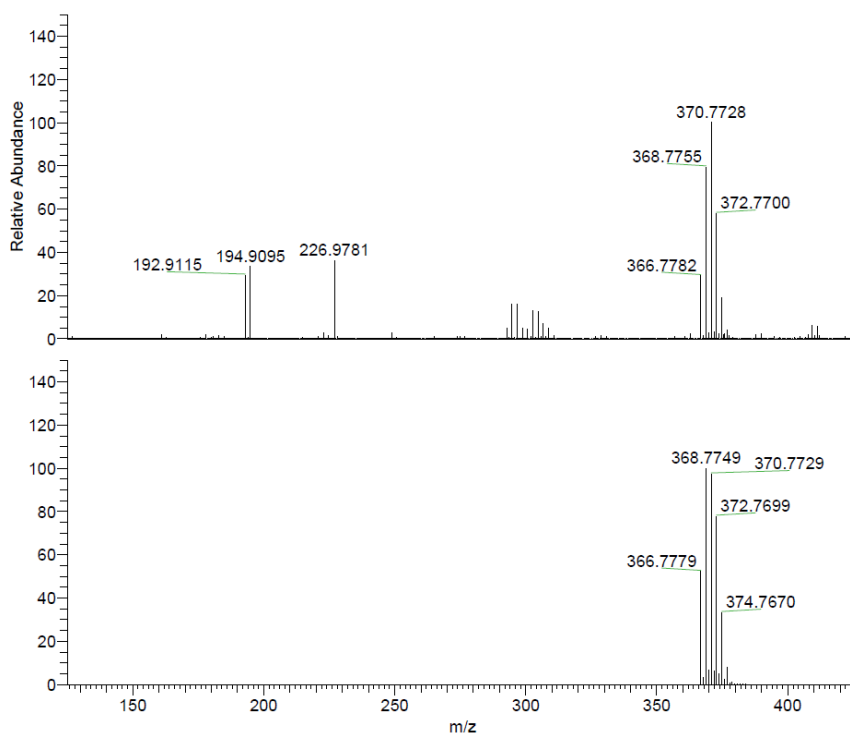


Figure 25. ESI(-)-HRMS spectrum of  $[\text{HCH}\cdot\text{Br}^-]$  complex. Comparison of the experimental spectrum (top) and simulated isotopic pattern (bottom).

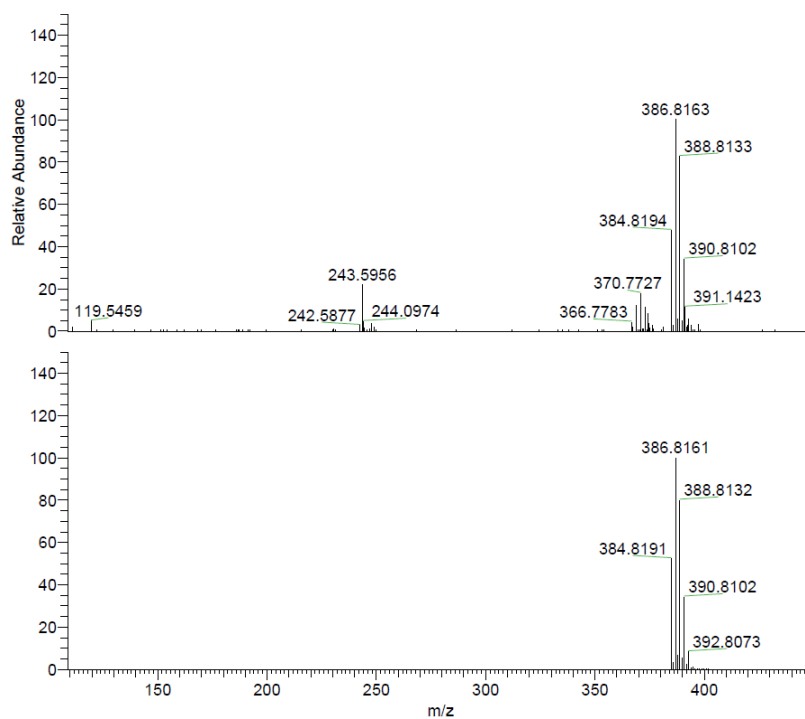


Figure 26. ESI(-)-HRMS spectra of  $[\text{HCH}\cdot\text{HSO}_4^-]$  complex. Comparison of the experimental spectrum (top) and simulated isotopic pattern (bottom).

### III. Conclusions

Solid state investigations proved that  $\beta$ -HCH acts as ditopic ligand for halide anions ( $\text{Cl}^-$  and  $\text{Br}^-$ ) and forms 3D supramolecular networks based on six axial  $\text{C}(\text{sp}^3)\text{-H} \cdots \text{X}^-$  contacts.

These interactions led to the obtaining of supramolecular polymers in which an important role of the pyridinium units was highlighted.

Investigations in solution [ $^1\text{H}$  NMR and ESI(-)-HRMS] revealed the formation of 1/1 complexes of  $\beta$ -HCH with all investigated anions.

The pattern of 1,3,5-three axial hydrogen atoms on a saturated six-membered ring decorated with electron withdrawing groups represents a powerful motif for anion recognition.

Our results unequivocally prove that  $\beta$ -HCH effectively and efficiently competes with more sophisticated structures for anion binding and we expect important applications such as anion transmembrane transport.

## Part C. Carbon Dots Based Innovative Photoluminescent Materials

### I.1. Introduction

In this chapter we focused our attention over a new area in the field of nanomaterials.

Carbon Quantum dots (CQDs), also known as carbon nanodots were discovered in the recent years and represent a new class of nanocarbon materials, with sizes under 10 nm.

Functionalized CQDs exhibit photoluminescence and this property have been already used for the obtaining of luminophores and in bioimaging<sup>28</sup>. The characteristics of CQDs are competing with those of semiconductors QDs, the advantages for CQDs being supported by the fact that they are cheaper and non-toxic<sup>29</sup>. Thus, the high yields reported in their synthesis, the stability and the photoluminescence properties of carbon quantum dots make them good candidates for applications in optoelectronics, as sensors, in photocatalysis, energy conversion<sup>30</sup> and others.

---

<sup>28</sup>Yang, S.-T., Cao, L., Luo, P.G., Lu, F., Wang, X., Wang, H., Meziani, M. J., Liu, Y., Qi, G., Sun, Y.-P. *J. Am. Chem. Soc.* **2009**, *131*, 11308-11309

<sup>29</sup>Yang, S.-T., Wang, X., Wang, H., Lu, F., Luo, P. G., Cao, L., Meziani, M. J., Liu, J.-H., Liu, Y., Chen, M., Huang, Y., Sun, Y.-P. *J. Phys. Chem. C.* **2009**, *113*, 18110-18114

<sup>30</sup>a) Yu, X., Liu, R., Zhang, G., Cao, H. *Nanotechnology* **2013**, *24*, 335401-335408; b) Zhang, Z., Zhang, J., Chen, N., Qu, L. *Energy Environ. Sci.* **2012**, *5*, 8869-8890; c) Cao, L., Sahu, S., Anilkumar, P., Bunker, C. E., Xu, J., Fernando, S., Wang, P., Gulians, E. A., Tackett, K. N., Sun, Y.-P. *J. Am. Chem. Soc.* **2011**, *133*, 4754-

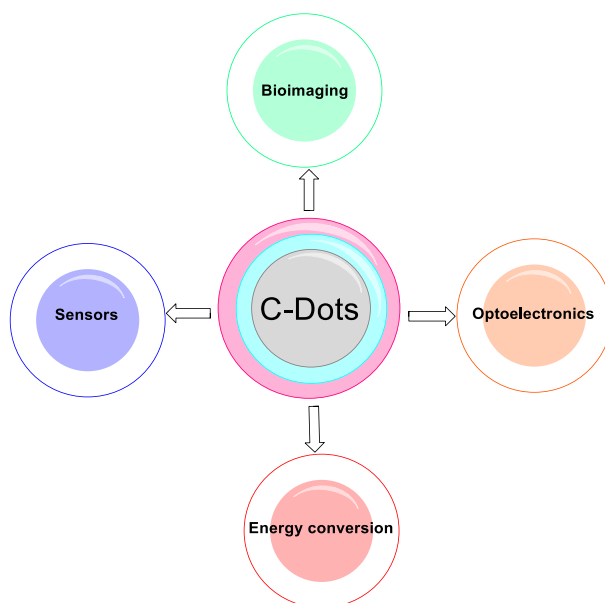


Figure 27. Applications of CQDs

Our purpose was to move toward functionalized CQDs modified with different monomers, oligomers or polymers in order to improve their photophysical properties and to investigate their potential applications as active materials in optoelectronic devices (CQD-LED) and solar cells (CQD-PV).

The methods envisaged in the obtaining of functionalized CQDs with polymers involved two strategies:

- **Grafting from**- obtaining of polymers and copolymers starting from the surface of CQDs

In “Grafting from” approach also named “host strategy” the conducting polymers are growing starting from the CQDs surface. By this method CQDs are included in the main chain of conducting polymers. In contrast to the strategy “grafting to”, on the surface of carbon nanoparticles will result a high grafting density of polymers. In this method the sizes of the nanoparticles can be controlled and the process can be shifted towards most efficient CQD.

- **Grafting to** – direct attachment of the polymers to surface of CQDs.

The ”grafting to” method or the “side chain functionalization” with conducting polymers, consist in direct grafting of derivatives of polythiophenes or poly(*para*-phenylenevinylene) on the surfaces of CQDs. The advantages of this method arise from the possibility of

---

4757; d) Sahu, S., Liu, Y., Wang, P., Bunker, C. E., Fernando, K. A. S., Lewis, W. K., Gulians, E. A., Yang, F., Wang, J., Sun, Y.-P. *Langmuir* **2014**, *30*, 8631–8636

polymerization of monomers by anionic, radical and cationic mechanism. The products exhibit narrow polydispersity and a small amount of polymer is directly immobilized on the surface of CQD, being a disadvantage of the method.

## **I.2. Objectives**

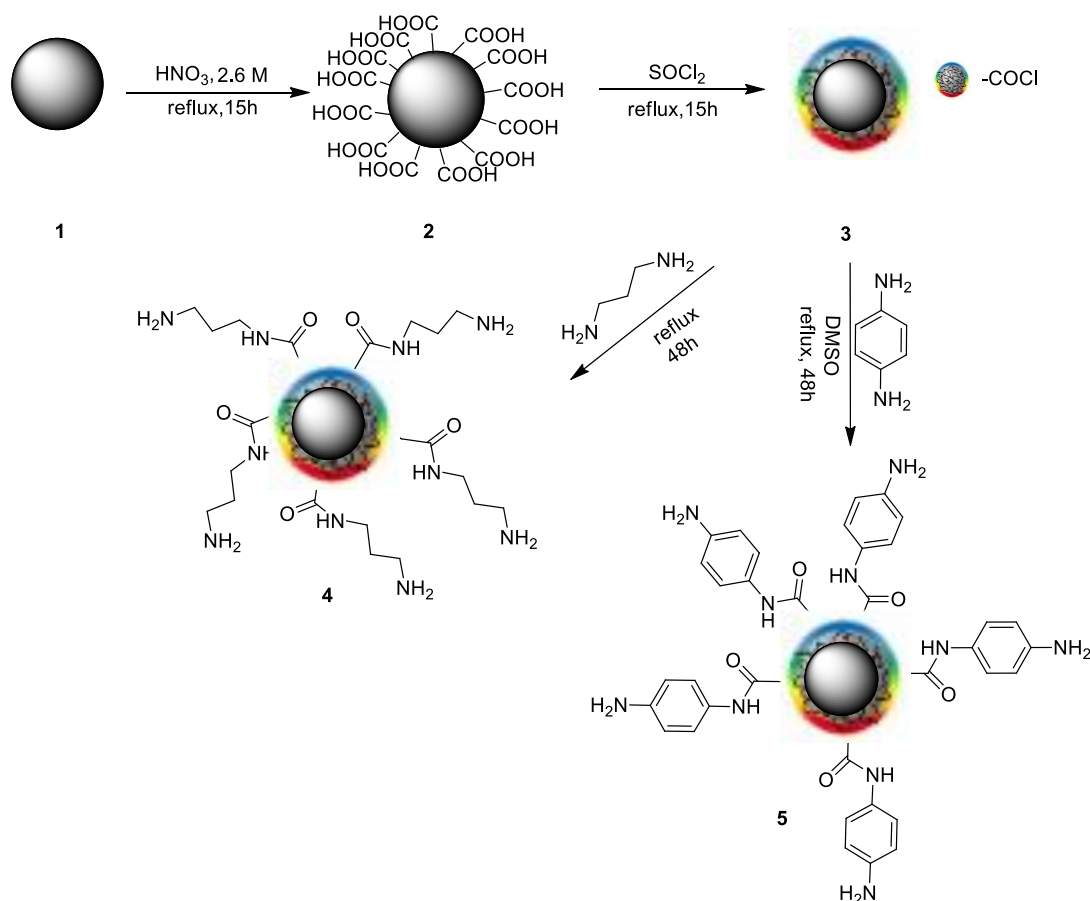
In the development of our research in the field of CQDs in order to obtain high performing materials for optoelectronic devices we followed two main directions:

1. The use of small molecules for the covering of the already functionalized surface of carbon nanoparticles
2. The use of “grafting-from” and “grafting to” polymerizations techniques, employing carbazole based monomers.

## **I.3. Grafting CQDs with small molecules**

Along this project, we propose to functionalize the surface of carbon nanoparticles with amide groups through an amide forming reaction using an aliphatic or aromatic diamine linker. To this end, a series of steps were followed.

The bare carbon nanoparticles (**1**) obtained by laser ablation were subjected in the first step to an oxidation reaction using 2.6 M aqueous solution of HNO<sub>3</sub> resulting in an oxidized nanocarbon particle covered with –COOH groups (**2**). The second step consisted in the activation of carboxy groups with SOCl<sub>2</sub>. In this step, some of the COOH groups were transformed into COCl groups resulting carbon nanoparticles covered with both COOH and COCl groups (**3**). This step is followed by treatment of (**3**), either with 1,3-propanediamine being obtained (**4**) or with *p*-phenylenediamine being obtained (**5**), nanoparticles covered with amide functions with aliphatic chains in (**4**) or aromatic ones in (**5**) (Scheme 20).



Scheme 20. Functionalization of CQDs (functionalized groups are represented illustrative only for a part of the aggregate)

Following this method we obtained CQDs of different sizes which were first separated by centrifugation and then by column chromatography using Sephadex G-100 as stationary phase, and ultrapure water as mobile phase. We separated three fractions (1-3) exhibiting a decrease in the sizes of the particles from fraction 1 to fraction 3.

Concerning reproducibility, the second batch of materials has led to lower fluorescence quantum yields and minor differences between different fractions were observed. The differences of QY (quantum yield) between different fractions are presented in Table 13. Very different QY for (4) is probably due to the smaller size of the particles because 1,3-propanediamine monomer led to functionalized nanoparticles mainly with smaller diameter. Microscope characterizations revealed in this case the presence of nanoparticles smaller than 5 nm (Figure 28)

Table 13. Fluorescence quantum yield of CQD-1,3- propanediamine.

CQD		Quantum yield (%)	
		375 nm	405 nm
<b>CQD-1,3- propanediamine</b>	Fraction 1	6.1	3.2
	Fraction 2	6.7	3.8
	Fraction 3	7.8	4.6

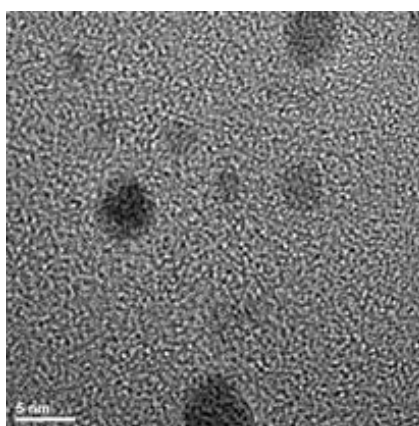


Figure 28. TEM image for CQDs functionalized with 1,3-propanediamine

The separated fractions, after excitation at different wavelengths (375-450 nm) show emissions in the range 450-520 nm. The fractions containing particles with smaller sizes exhibited a quantum yield of 8% in the case of the functionalization of CQDs with 1,3-propanediamine (Figure 29a) while, if the functionalization was carried out using *p*-phenylenediamine, these fractions had lower quantum yield of 3% (Figure 29b).

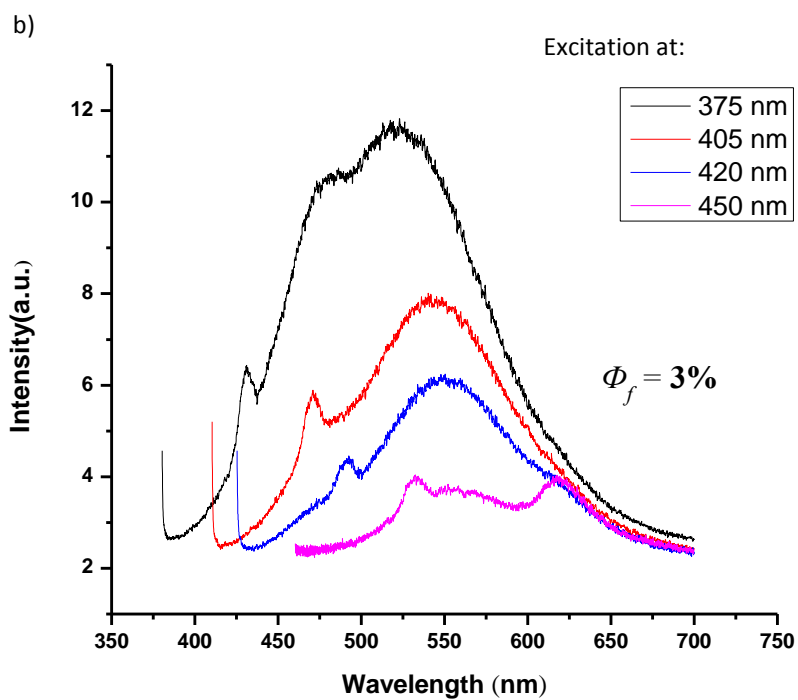
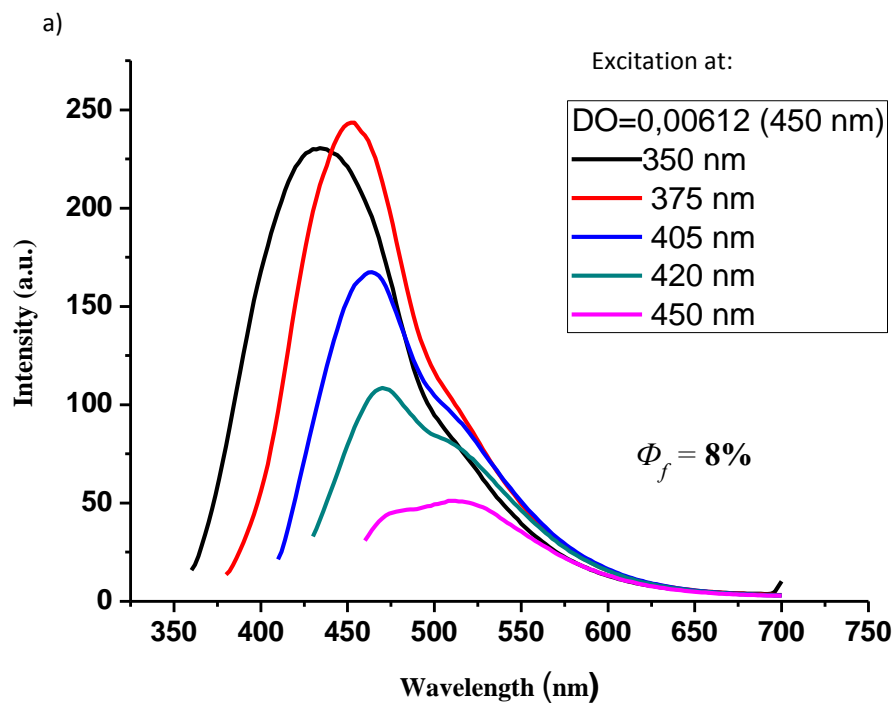
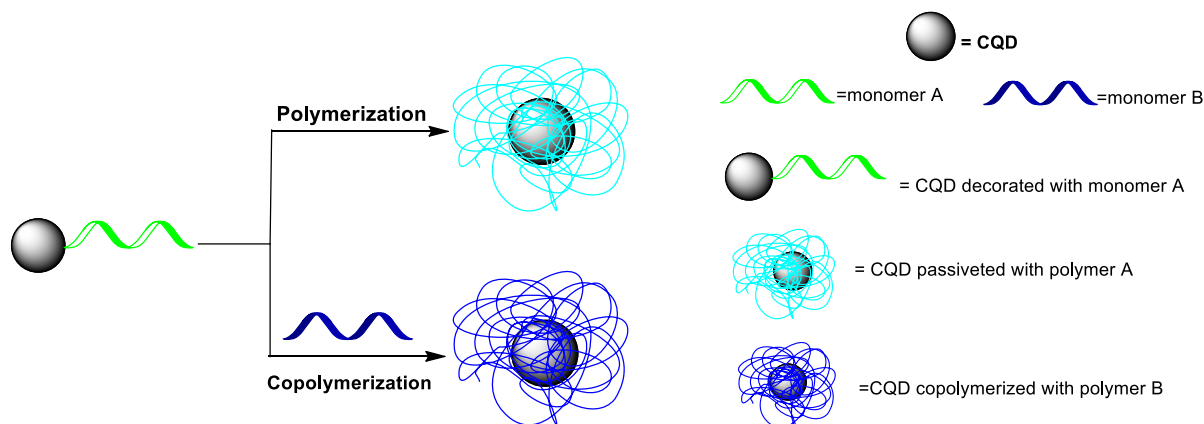


Figure 29. a) Emission spectra of CQDs with 1,3-propanediamine; b) Emission spectra of CQDs with *p*-phenylenediamine.

#### I.4. Functionalization of carbon nanoparticles with oligomers or polymers

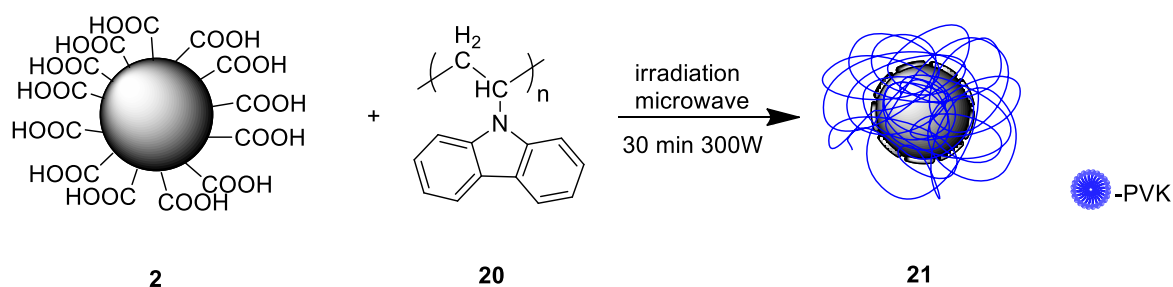
Generally in “grafting from” method, CQDs are incorporated in the polymer starting the polymerization from the surface of CQDs by modulating the attachment of the monomer. A second monomer (various structures) can be introduced for copolymerization (Scheme 21).



Scheme 21. "Grafting from" method for preparing polymer-functionalized CQDs

#### I.5. Microwave functionalization of carbon nanoparticles

Another way to carry out the passivation of carbon nanoparticles with oligomeric carbazole units, consisted in reacting, in field of microwaves, the carbon nanoparticles covered with COOH groups (**2**), (Scheme 20) with commercially available poly(vinylcarbazole) (PVK, Scheme 22) or *N*-vinyl carbazole (NVK, Scheme 23).



Scheme 22. Passivation of CQDs with PVK

In a series of reactions polyvinylcarbazol (PVK) and carboxyl group decorated carbon nanoparticles (CNP) were blended together under stirring in a pre-heated oven for 30 minutes at 300W. The reaction product was brought to room temperature, dispersed in THF, and



centrifuged at 20000xg for one hour. The optical absorption spectrum of the obtained PVK-carbon dots (**21**) is shown in figure 31.<sup>31</sup>

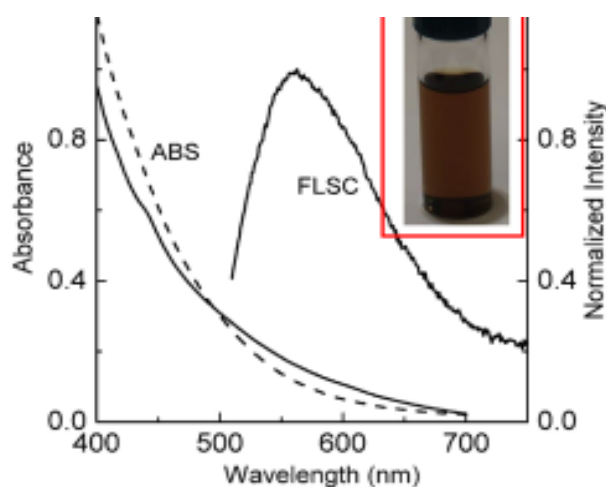


Figure 30. Absorption (ABS) and fluorescence (FLSC) (500 nm excitation) spectra of PVK-carbon dots (**21**) in THF solutions (--) and the absorption spectrum of aqueous suspended precursor carbon nanoparticles (-), (represented from reference 31)

As the photoluminescence emissions and the fluorescence maxima of the PVK-carbon dots (**21**) are wavelength dependent (Figure 30)<sup>31</sup>, a confirmation of the correct values of our experimental results came from their similarity to previous reports in the literature<sup>32,33,34</sup>

At longer excitation wavelengths, the carbon dots emission was progressively red-shifted and revealed narrowing of the spectra bands widths. The excitation wavelength dependence of the carbon dots displays full coverage of the visible spectra. The photoluminescent quantum yields were calculated to be 13% at 400 and 440 nm using 9,10-bis(phenylethynyl)anthracene as a standard, which has a quantum yield of 100% as determined by calibration against quinine sulphate standard.<sup>35</sup>

The morphological characterization by transmission electron microscopy (TEM), was done with carbon dots deposited onto a holey-carbon TEM grid. Representative TEM images are shown in figure 31.

<sup>31</sup>Rednic, M. I., Lu, Z., Wang, P., LeCroy, G. E., Yang, F., Liu, Y., Qian, H., Terec, A., Veca, L. M., Lu, F., Sun, Y.-P. *Chem. Phys. Lett.* **2015**, 639, 109-113

<sup>32</sup>Li, H., He, X., Kang, Z., Huang, H., Liu, Y., Liu, J., Lian, S., Tsang, C. H., Yang, X., Lee, S. T. *Angew. Chem. Int. Ed.* **2010**, 49, 4430-4434

<sup>33</sup>Wang, Y., Hu, A. *J. Mater. Chem. C* **2014**, 2, 6921-6939

<sup>34</sup>LeCroy, G. E., Sonkar, S. K., Yang, F., Veca, L. M., Wang, P., Tackett, K. N., Sun, Y.-P. *ACS Nano* **2014**, 8, 4522-4529

<sup>35</sup>Bunker, C. E., Sun, Y.-P. *J. Am. Chem. Soc.* **1995**, 117, 10865-10870

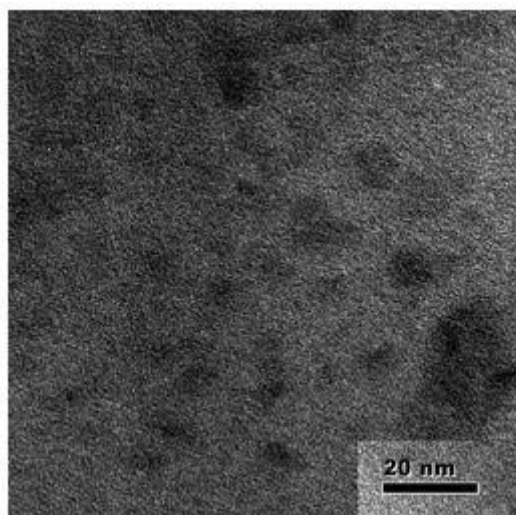


Figure 31. TEM images for specimen of the PVK-carbon dots (represented from reference 31) Polymer functionalization has also been done by thermal treatment of a mixture of solutions of PVK/CQDs in DMF. The mixed solutions were vigorously stirred, followed by partial solvent evaporation under N<sub>2</sub>. Then the resulted mixture was irradiated in the microwave for 30 minutes at 300 W. After cooling at room temperature, the solid was dispersed in THF and centrifuged at 20000xg for one hour, resulting in a highly collared solution of PVK/CQDs.

In the past few years, PVK was utilized as a material for non-volatile organic memory applications, due to its bistable resistance<sup>36</sup> behaviour in multi-layers structures based on PVK films.

The synthesized PVK-carbon dots samples made them ideal for the fabrication of PVK-carbon dots films. In a typical experiment for film with high carbon dot content, a solution of PVK-carbon dots and neat PVK in solvent mixture of chlorobenzene / chloroform (3/1, v/v) were prepared. The sample was vigorously stirred, followed by slow solvent evaporation, which resulted in a polymer blend. The concentrated solution was drop-cast onto a pre-cleaned glass substrate and allowed to dry in ambient conditions for 12 hours, after that the film could be peeled off from glass for characterization; the thickness of the film was around 5 μm (Figure 32).

---

<sup>36</sup> Lai, Y.-S., Tu, C.-H., Kwong, D.-L. *Appl. Phys. Lett.* **2005**, 87, 122101, 1-3

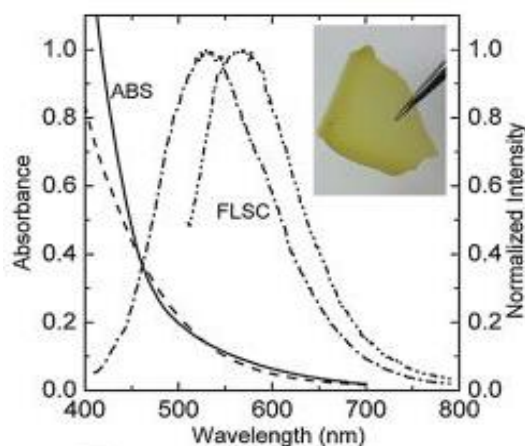
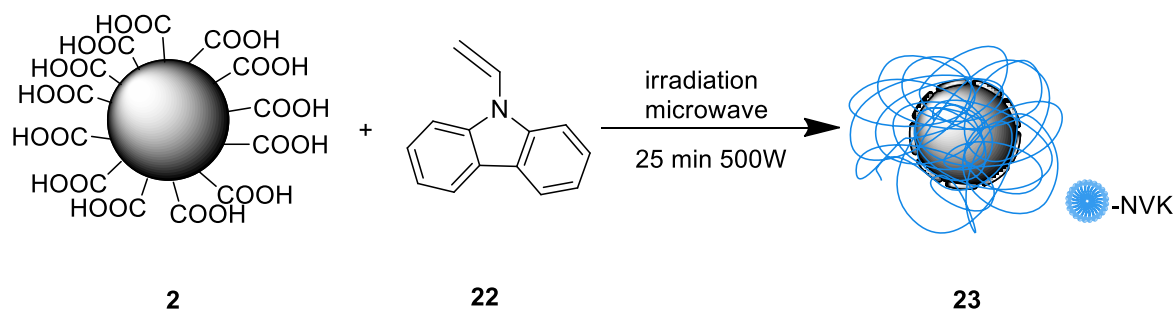


Figure 32. Absorption (ABS ---) and fluorescence (FLSC, with excitation at 400 nm -.-.-and 500 nm -.-.-) spectra for the film of PVK-carbon dots+PVK, with the absorption of aqueous suspended carbon nanoparticles also shown for comparison; insert: photograph for a typical film (represented from reference 31)

The film containing PVK and carbon particles, exhibited similar optical absorption and fluorescence emissions to those of the PVK-carbon dots in solutions (Figure 30).

In the same conditions described for the solid polyvinylcarbazole (PVK), mechanically mixed NVK (*N*-vinyl carbazole) and CQD powders (**2**) were irradiated in a preheated microwave oven for 25 minutes at 500 W (Scheme 23). The sample was cooled to room temperature in air, dispersed in THF and centrifuged at 20000xg for 1 hour, resulting carbon nanoparticles functionalized with NVK moieties (**23**).



Scheme 23. Functionalization of CQDs with NVK

The fluorescence quantum yield (QY) of the NVK-carbon dots **23** in THF solutions, at 420 nm excitation was around 20%, a result comparable with PEG<sub>1500N</sub>- carbon dots (with QY 10-20%, in aqueous solutions)<sup>37</sup>

<sup>37</sup>Wang, X., Cao, L., Yang, S., T. Lu, F., Meziari, M. J., Tian, L., Sun, K. W., Bloodgood, M. A., Sun, Y.-P. *Angew. Chem. Int. Ed.* **2010**, *49*, 5310-5314.

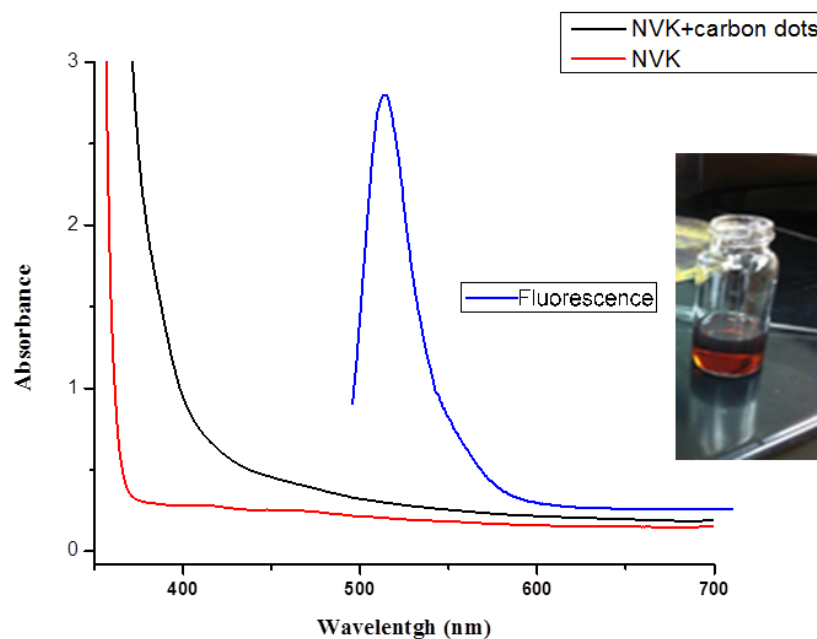


Figure 33. Absorption spectra for NVK(-), NVK + carbon dot **23** (-) and fluorescence (-) [excitation at 420 nm for NVK+carbon dots **23**]; insert: photograph for solution of NVK+carbon dots **23**

In these experiments we used the carbon dots as an initiator to polymerization of NVK (*N*-vinyl carbazole) under microwave irradiation.

Through this one-pot thermo-chemical method of passivation of the surface of carbon dots with PVK or NVK we have obtained materials with high quantum yields, a property necessary for optoelectronics devices.

Further studies and more detailed analysis on the reaction mechanism based on microwave irradiation are required.

## II. Conclusions

Novel functionalized carbon nanoparticles with optimized optoelectronics properties were obtained by the decoration of the surface area of carbon nanoparticles with aromatic or aliphatic small organic molecules, different oligomers and polymers obtained through classical organic synthesis and by one-pot thermal irradiation in microwave field.

The functionalized carbon nanoparticles were submitted to size separations of CQDs (by centrifugation and Sephadex chromatography), the properties of CQDs were size dependent the best photoluminescent properties being recorded for the particles with the smallest size distribution ( $d < 5$  nm)

The optical properties of carbon dots obtained by thermochemical synthesis are in line with those obtained from chemical functionalization method.

Surface modification of carbon nanoparticles with different molecules opens new opportunities for further investigations in order to obtain new CQDs with better photoluminescent properties.

### **General conclusions**

This thesis brought important contributions in different fields as supramolecular chemistry, organic synthesis, anion sensing and material science.

An original method based on the nucleophilic aromatic substitution reactions was developed for the successful synthesis of cyclophanes and cryptands with phenothiazine bridges. These compounds revealed remarkable ability for the complexation of organic and cationic guests. The emission spectra of the investigated supramolecular systems obtained by the complexation of cyclophanes with  $\text{Cd}^{2+}$  and  $\text{Pb}^{2+}$  allowed the conception of a XOR molecular logical gate.

The investigation of several dynamic constitutional libraries obtained from phenothiazine based dialdehydes and bismethylaminobenzenes revealed the evaluation of these dynamic systems towards unique macrocyclic compounds (either a dimer macrocycle or a catenane).

The anions recognition by a simple molecule ( $\beta$ -HCH) was studied in solid state and in solution. The single crystal X ray diffraction investigations revealed the formation of supramolecular polymers and the difacial complexation of  $\beta$ -HCH by  $\text{Cl}^-$  and  $\text{Br}^-$  by exciting  $\text{C}(\text{sp}^3)\text{-H} \cdots \text{anion}$  contacts. The remarkable values of the stability constants of the 1 / 1 complexes  $\beta\text{-HCH} / \text{anion}$  were calculated using  $^1\text{H}$  NMR titrations.

Several original materials were obtained by the functionalization of CQDs with small molecules, oligomers and polymers and then their photochemical properties were investigated by appropriate methods. The synthesis of an efficient photoluminescent material with remarkable quantum yields emission was obtained by microwave assisted functionalization of C-dots with vinylcarbazole.

## *List of Publications*

### **1. Supramolecular anion recognition by $\beta$ -HCH**

Monica I. Rednic, Richard A. Varga, Attila Bende, Ioana G. Grosu, Maria Miclăuș, Niculina D. Hădăde, Anamaria Terec, Elena Bogdan and Ion Grosu *Chem. Commun.*, **2016**, Accepted Manuscript, doi: 10.1039/C6CC06842

**Impact factor (2016): 6.56**

**Red zone: Chemistry Multidisciplinary**

### **2. Fluorescent carbon ‘quantum’ dots from thermochemical functionalization of carbon nanoparticles**

Monica I. Rednic, Zhuomin Lu, Ping Wang, Gregory E. LeCroy, Fan Yang, Yun Liu, Haijun Qian, Anamaria Terec, L. Monica Veca, Fushen Lu, Ya-Ping Sun *Chem. Phys. Lett.* **2015**, 639, 109-113, doi:10.1016/j.cplett.2015.08.069.

**Impact factor (2015): 1.89**

**Yellow zone: Physic, Atomic, Molecular and Chemical**

### **3. Podands with 3,7,10-Trisubstituted Phenothiazine Units: Synthesis and Structural Analysis**

Monica I. Rednic, Szabolcs Szima, Elena Bogdan, Niculina D. Hădăde, Anamaria Terec and Ion Grosu *Rev. Roum. Chim.* **2015**, 60, 637-642

**Impact factor (2015): 0.31**

### **4. Macrocycles embedding phenothiazine or similar nitrogen and/or sulphur containing heterocycles**

Monica I. Rednic, Niculina D. Hădăde, Elena Bogdan, Ion Grosu *J. Incl. Phenom. Macrocycl. Chem.* **2015**, 81, 263-293, doi 10.1007/s10847-014-0455-x

**Impact factor (2015): 1.25**

**Yellow zone: Chemistry Multidisciplinary**

### **5. Cryptands with 1,3,5-Tris(1',3'-dioxan-2'-yl)-benzene Units: Synthesis and Structural Investigations**

Monica Cîrcu, Albert Soran, Niculina Daniela Hădăde, Monica Rednic, Anamaria Terec, Ion Grosu *J. Org. Chem.* **2013**, 78, 8722–8729, dx.doi.org/10.1021/jo401432y

**Impact factor (2013): 4.63**

**Red zone: Chemistry Organic**

## *Scientific Communications*

1. **Oral presentation** at Iasi Academic Days “**Progress in organic and polymer chemistry**” XXIVnd Edition, 3-5 october 2013 Iasi, Romania
2. **Oral presentation** at Iasi Academic Days “**Progress in organic and polymer chemistry**” XXVnd Edition, 24-26 september 2015 Iasi, Romania

**Research Stage:** 02.09.2014 – 30.11.2014

Clemson University, Department of Chemistry, College of Engineering and Science 219  
Howard L. Hunter Chemistry Laboratory, South Carolina  
(Dr. Ya-Ping Sun)